All ETDs from UAB

UAB Theses & Dissertations

2015

Carbon Fiber Content Measurement In Composite

Qiushi Wang
University of Alabama at Birmingham

CARBON FIBER CONTENT MEASUREMENT IN COMPOSITE

by

QIUSHI WANG

HAIBIN NING, CHAIR
UDAY VAIDYA
SELVUM PILLAY
MARK WEAVER
ALAN EBERHARDT

A DISSERTATION

Submitted to the graduate faculty of The University of Alabama at Birmingham,
in partial fulfillment of the requirements for the degree of
Doctor of Philosophy

BIRMINGHAM, ALABAMA

2015

CARBON FIBER CONTENT MEASUREMENT IN COMPOSITE

QIUSHI WANG

MATERIALS ENGINEERING

ABSTRACT

Carbon fiber reinforced polymers (CFRPs) have been widely used in various structural applications in industries such as aerospace and automotive because of their high specific stiffness and specific strength. Their mechanical properties are strongly influenced by the carbon fiber content in the composites. Measurement of the carbon fiber content in CFRPs is essential for product quality control and process optimization. In this work, a novel carbonization-in-nitrogen method (CIN) is developed to characterize the fiber content in carbon fiber reinforced thermoset and thermoplastic composites. In this method, a carbon fiber composite sample is carbonized in a nitrogen environment at elevated temperatures, alongside a neat resin sample. The carbon fibers are protected from oxidization while the resin (the neat resin and the resin matrix in the composite sample) is carbonized under the nitrogen environment. The residue of the carbonized neat resin sample is used to calibrate the resin carbonization rate and calculate the amount of the resin matrix in the composite sample. The new method has been validated on several thermoset and thermoplastic resin systems and found to yield an accurate measurement of fiber content in carbon fiber polymer composites.

In order to further understand the thermal degradation behavior of the high temperature thermoplastic polymer during the carbonization process, the mechanism and the kinetic model of thermal degradation behavior of carbon fiber reinforced poly (phenylene sulfide) (CPPS) are studied using thermogravimetry analysis (TGA). The CPPS is subjected to TGA in an air and nitrogen atmosphere at heating rates from 5 to 40°C min^{-1}. The TGA curves obtained in air are different from those in nitrogen. This demonstrates that weight loss occurs in a single stage in nitrogen but in two stages in air. To elucidate this difference, thermal decomposition kinetics is analyzed by applying the Kissinger, Flynn-Wall-Ozawa, Coat-Redfern and Malek methods. The activation energy (E_a) of the solid-state process is determined to be 202 kJ mol^{-1} in an oxidative atmosphere using Kissinger's method, which is 10-15 kJ mol^{-1} more than the results calculated in a nitrogen atmosphere. The value of the activation energy obtained using Ozawa-Flynn methods is in agreement with that using the Kissinger method. Different degradation mechanisms are used to compare with this value. Based on the analytical result, the actual thermal degradation mechanism of the CPPS is a D_n deceleration type. The carbonization temperature range of the CPPS is the same as pure PPS resin.

Keywords: carbon fiber content, thermoset, thermoplastic, thermal degradation

DEDICATION

To my beloved parents for their constant support and guidance.

ACKNOWLEDGMENTS

Table of Contents

LIST OF TABLES

DETERMINATION OF THERMAL DEGRADATION KINETIC PARAMETERS OF
CARBON FIBER REINFORCED PPS USING TGA

LIST OF FIGURES

MEASUREMENT OF THE FIBER CONTENT OF CARBON FIBER REINFORCED
THERMOPLASTIC COMPOSITES USING CARBONIZATION-IN-NITROGEN
METHOD

DETERMINATION OF THERMAL DEGRADATION KINETIC PARAMETERS OF
CARBON FIBER REINFORCED PPS USING TGA

1. GENERAL INTRODUCTION

A composite structure is a combination of two or more different constituents that can be physically distinguished, resulting in a final product that has better performance than each individual constituent. Composite materials consist of a matrix (polymer, metal or ceramic) and one or more reinforcing phases (fibers, particles, flakes or fillers). The different constituents are combined judiciously to achieve a system with better structural or functional properties than can be attained by any of the constituents alone. Composites are becoming an essential part of today's materials due to advantages such as low weight, strong corrosion resistance, high fatigue strength, and faster assembly. They are extensively used as materials in making aircraft structures, electronic packaging, medical equipment, space vehicles, and home-building supplies [1].

The separate constituents in a composite are normally named as matrix and dispersed phased. The matrix phase is the primary phase having a continuous character. The matrix is usually the more ductile and less hard phase. It holds the dispersed phase and shares a load with it. The dispersed (reinforcing) phase is embedded in the matrix in a discontinuous form. The dispersed phase is usually stronger than the matrix, therefore, it is sometimes called the reinforcing phase.

Composites in structural applications have the following characteristics:

- They generally consist of two or more physically distinct and mechanically separable materials.

- They are made by mixing the separate materials in such a way as to achieve controlled and uniform dispersion of the constituents.

- They have superior mechanical properties and in some cases uniquely different form the properties of their constituents.

Depending on the matrix material, composites can be classified as metal matrix composites (MMCs), ceramic matrix composites (CMCs), or polymer matrix composites (PMCs) [2]. The classification according to types of reinforcement are particulate composites (composed of particles), fibrous composites (composed of fibers), and laminate composites (composed of laminates).

1.1 Polymer matrix composites

Polymer matrix composites (PMCs) are commonly defined as a composite which is comprised of a variety of short or continuous fibers bound together by an organic polymer matrix. The reinforcement in a PMC provides high strength and stiffness. The PMC is designed so that the mechanical loads to which the structure is subjected in service are supported by the reinforcement. The function of the matrix is to bond the fibers together and to transfer loads between them. Polymer matrix composites (PMCs) have evolved and gained prominence over metals due to their specific strength, specific stiffness, corrosion resistance, acoustical dampening, and tailorability. The versatility of the material is also enhanced by the wide range of choices available for the types of reinforcement and matrices to meet demands in engineering, biomedical, and other applications [3-5].

Polymer matrices in PMCs are classified in two categories: thermoset and thermoplastic. In the thermoset polymers, the molecules are cross-linked due to a chemical reaction during the curing process. Once cross-linked, thermoset resins are permanently set and tend to chemically decompose at elevated temperatures. Thermoset resins include polyesters, vinyl esters and epoxies. Thermoset polyesters are commonly used in fiber-reinforced plastics, and epoxies make up most of the current market for advanced composites resins. Initially, the viscosity of these resins is low; however, during curing thermoset resins undergo chemical reactions that crosslink the polymer chains and thus connect the entire matrix together in a three-dimensional network. Thermosets, because of their three-dimensional cross-linked structure, tend to have high dimensional stability, high-temperature resistance, and good resistance to solvents.

3

Thermoplastic resins include polypropylene (PP), polyamide imide (PA), poly (phenylene sulfide) (PPS) and poly (ether ether ketone) (PEEK). These consist of long, discrete molecules that melt to a viscous liquid at the processing temperature, typically 20 to 360°C, and, after forming, are cooled to an amorphous, semi-crystalline, or crystalline solid. Unlike the curing process of thermosetting resins, the processing of thermoplastics is reversible. By simply reheating to the process temperature, the resin can be formed into another shape if desired. Thermoplastic polymers are characterized by linear chain molecules that can soften and be repeatedly reprocessed. The heating or cooling cycle can be repeated many times, thus giving the product an almost indefinite shelf life.

Fiber-reinforced polymer composites exhibit high specific strength, specific stiffness and corrosion resistance compared to conventional metallic components. They have gained prominence over traditional materials with their versatility and superior performance, thus widely being preferred in aerospace, automotive, marine and sporting applications. The fiber reinforcements of the PMCs consist of glass, carbon, or aramid fibers. Glass fiber is the most widely-used reinforcement for structural plastics due to its high elastic modulus and high strength, while carbon fiber has become more and more popular in the aircraft and spacecraft industries for its weight benefits and more affordable cost. Carbon fiber reinforcement also shows high strength, stiffness and modulus. In a carbon fiber reinforced composite, the fibers serve as a load-carrying member. The matrix protects the fibers from the environment and also acts as a load transfer medium between fibers. Carbon fiber reinforced polymers (CFRPs) are predominately used in advanced aerospace applications [6-10].The Boeing 787 Dreamliner, for example, takes advantage of

4

advanced composite materials by using 50% of polymer composites by weight in its design.

1.2 Fabrication of polymer matrix composites

The important processing methods are hand lay-up, bag molding, filament winding, pultrusion, bulk molding, sheet molding, resin transfer molding, injection molding, and so on.

For preparing thermoset composites, hand lay-up is one of the simplest and oldest molding methods for the manufacture of both small and large reinforced products. In this method, the reinforcing mat or woven fabric or roving is positioned manually in the open mold, and the resin is poured, brushed, or sprayed over and into the reinforcements. The entrapped air is removed manually with squeegees or rollers to complete the laminate structure. Room temperature curing polyesters and epoxies are the most commonly used matrix resins. Curing is initiated by a catalyst in the resin system, which hardens the fiber-reinforced resin composites without external heat. The fiber content of a composite sample processed by hand layup process can be well controlled. The dry fabrics are firstly weighed and then the cured composite is weighed. Care is taken to ensure that there is no loss or gain of any fiber during the processing. The ratio of the dry fabric mass to the composite mass is the fiber content of the composite. The hand layup process is used to prepared carbon-fiber-reinforced thermoset composite samples in this work.

Hot-melt impregnation is a continuous composite processing method that impregnates fibers with thermoplastic resin. It produces intermediate forms, such as unidirectional tape or long fiber reinforced thermoplastic (LFT) rods. Fiber tows pass through a thermoplastic resin bath (in a heating die) in which the fibers are impregnated and coated

with the resin. Then, the coated fibers are pulled by a puller and go through several heating rollers to scrap the extra resin. It is then cooled down to form the unidirectional tape or to be chopped into desired length for LFT application. Fast production speed can be achieved by this technique. It is a process method that could accurately control the fiber content of the thermoplastic unidirectional tapes. The fiber content of the composite tape can be measured by weighing the dry fiber tow with a certain length (for example 20 cm) and the composite tape with the same length. The difference of the dry fiber tow mass and the composite tape mass is completely attributed to the resin coated on the fibers. The fiber content of the composite tape is calculated to be the ratio of the dry fiber tow mass to the composite tape mass. In this study, the hot melt impregnation process is used to prepare the thermoplastic composite samples needed for validating the CIN method.

1.3 Factors affecting properties of CFRPs

The mechanical properties of carbon fiber reinforced polymer composites highly depend on several factors: the presence of defects, the binding force between the carbon fiber and the resin, and the carbon fiber content and its distribution in the thermoplastic resin. The fiber-matrix interfacial adhesion plays an important role in determining the mechanical propertied of a PMC. Chen and Curliss (2001) found out that a better interfacial bond will result in better properties of a fiber reinforced composite [11, 12]. While the in-plane, fiber-dominated properties (for example tensile strength) make these composites highly desirable as compared to metals, their thickness direction properties are limited by the performance of the matrix resin. However, their compressive strength is generally much lower due to the fact that under compression, the fibers tend to fail through buckling well

6

before a compressive fracture occurs. In addition, fiber misalignment and the presence of voids during the manufacturing processes contribute to a further reduction in compressive strength. In fact, the overall compressive strength of a polymer matrix composite is only about 50% of its tensile strength. The strength of the surrounding polymer matrix plays a key role in characterizing the critical buckling load of the fibers. It has been found the fiber content and its distributions are the most important factors in determining the mechanical properties of fiber-reinforced polymers. Smith et al (2007), Chen et al (1999) and Simon et al (1987) have studied the effect of fiber content on the resulting properties of composite materials [13-15]. They found that the carbon fiber is served as the primary reinforcement to provide strength and stiffness composites. The shear and tensile properties are extremely dependent on the fiber content and hence very sensitive to local fiber variations that arise during processing. Therefore the magnitude of deviation of carbon fiber content values in CFRP composites for practical use in aircraft and cars must be lower than a certain value [16, 17].

1.4 Carbon fiber content measurement methods

Literature reviews have highlighted several analysis methods that have been used to measure the carbon fiber content in composites.

The most common methods for measuring the carbon fiber content in composites are described by ASTM D3171-Standard Test Methods for Constituent Content of Composite Materials [34]. It includes two ways to measure the fiber content by removing the matrix from the composites: matrix burn-off in air and matrix digestion. The matrix burn-off method utilizes a furnace to degrade and remove the matrix from the composite, facilitating measurement of the fiber weight fraction. Fiber degradation will affect the

accuracy of this technique, because fiber mass can also be degraded or removed. This error is especially prevalent for composites with high temperature thermoplastic resin (PPS, PEI, PEEK) matrices, because the temperatures needed for burning the matrix (decomposing temperature > 500°C) are above carbon fiber oxidizing temperature [18-20]. Matrix digestion is similar to matrix burn-off, except that acid is used to digest and remove the matrix from the composite instead of using thermal degradation. Specimen preparation can be time-consuming, since samples are normally ground to small particle sizes to ensure larger contact areas between the polymer and the acid. Toxic fumes are also generally produced during the chemical break down of the matrix, posing hazards to the environment and the test operators.

Another method is optical microscopy analysis [38]. In this case, slices of the specimens are analyzed by two-dimensional image processing to determine the fiber content. This may also lead to misrepresentation from studying three-dimensional features (fiber volume/weight content) using a two-dimensional characterization method (fiber area on a polished surface). To get sufficiently accurate results, a large number of areas have to be analyzed. This approach is not practical as specimen preparation and image analysis are extremely time consuming and expensive. For discontinuous fiber-reinforced composites, the inhomogeneous distribution of carbon fiber will amplify the inaccuracy level of the results derived from the limited number of analyzed slices.

Thermogravimetric Analysis (TGA) could also be used to measure the carbon fiber content, as reported by Polis [21]. In this method, a sample weighing less than 0.1 gram is used. However, this small sample size is not sufficiently representative of carbon fiber composite structures. The TGA method has not been widely adopted because of the low

confidence level derived from using small sample size (0.1 gram) to represent large composite structures. Both the microscopy and TGA methods are limited in their accuracy and reliability.

1.5 Mechanisms of thermal degradation of polymers

Depolymerization and statistical fragmentation of chains are generally the two mechanisms of degradation of polymers. The rate and extent of degradation may be monitored by changes in a sample's mass and molecular weight, detection and quantification of reaction enthalpy changes, quantitative analysis of reaction by-products such as carbonyls and/or measurement of oxygen consumption. The factor that limits polymer thermal stability is the strength of the weakest bond in the polymer chain. Thermal degradation of polymers can follow three major pathways: side-group elimination, random scission, and depolymerization [22, 23].

Side-group elimination

Side-group elimination takes place generally in two steps. The first step is the elimination of side groups attached to a backbone of the polymer. This leaves an unstable polymer macromolecule that undergoes further reactions, including the formation of aromatic molecules, scission into smaller fragments, or the creation of char. The first step of thermal degradation of PVC, for example, is the elimination of the side groups to form hydrogen chloride. With the side groups removed, a polyene macromolecule remains. This then undergoes reaction to form aromatic molecules, typically benzene, toluene and naphthalene.

Random scission

Random scission involves the formation of a free radical at some point on the polymer backbone, producing small repeating series of oligomers, usually differing in chain length by the number of carbons. The fragmentation of polyethylene produces molecules with a double bone at one end, and molecules containing two double bones located at either end of molecule. Polymers that do not depolymerize, like polyethylene, generally decompose by thermal stress into fragments that break again into smaller fragments and so on. The degree of polymerization decreases without the formation of free monomeric units. Statistical fragmentation can be initiated by chemical, thermal or mechanical activation or by radiation.

If such random scission events are repeated successively in a polymer and its degradation products, the result is initially a decrease in molecular weight and ultimately weight loss, as degraded products with a broad range of carbon numbers become small enough to evaporate without further cleavage.

Depolymerization

Depolymerization is a free-radical mechanism in that the polymer is degraded into the monomer or comonomers that make up the polymer. Several polymers degrade by this mechanism, including polymethacrylates and polystyrene. The formation of a free radical on the backbone of the polymer causes the polymer to undergo scission to form unsaturated small molecules and propagate to the free radical on the polymer backbone. The mechanism of depolymerization can occur under the same condition (high temperature) as statistical fragmentation. Several polymers can be depolymerized until

the equilibrium between monomer and polymer at a given temperature is reached in a closed reaction system.

In most of cases, the three degradation pathways happen at the same time in a degradation process. Different pathways dominate at different temperature ranges based on the structure of the polymers. At the end of the degradation process, the carbonization process is normally the dominating degradation behavior, especially in inert atmospheres. In this process, the polymer chain transfer to a variety of products by forming the char at a high pyrolysis temperature. The residue weight appeared to remain constant.

1.6 Kinetics of thermal degradation

Generally, the thermal degradation of polymeric materials follows more than one mechanism. The existence of more than one concurrent chemical reaction accompanied by other physical phenomena such as evaporation and ablation introduce further complications for the modeling of degradation kinetics. Kinetic study of thermal degradation provides useful information for the optimization of the successive treatment of polymer materials, in order to avoid or at least limit thermal degradation. The analysis of the degradation process becomes more and more important due to an increase in the range of temperatures for engineering applications and for the recycling of post-consumer plastic waste.

By far the most valuable approach for measuring thermal degradation kinetic parameters is thermogravimetric analysis (TGA). In TGA experiments, the sample is brought quickly up to the desired temperature and the weight of the sample is monitored during the course of thermal decomposition. By employing the TGA results (plot of weight vs. Temperature) with different methods, the kinetic parameters can be extracted and

calculated. Those kinetic parameters can then be used to predict the thermal degradation type of the polymer.

The general form of the kinetic expression used in analyzing dynamic and isothermal TGA data is based on order reaction mechanism and in most cases, all kinetic studies assume that the isothermal rate of conversion[24], $d\alpha/dt$ which could be described as follow:

$$\frac{da}{dt} = kf(\alpha) \tag{1}$$

Where α is the reaction rate, which is defined as the derivative of the conversion with respect to time. $f(\alpha)$ depends on the mechanism of the degradation reaction. The function k is described by the Arrhenius expression:

$$k = Ae^{-\frac{E}{RT}} \tag{2}$$

Where A, the pre-exponential factor (min^{-1}), E_a is assumed to be independent of temperature, is the activation energy (kJ mol^{-1}), is the absolute temperature (K) and R is the gas constant ($8.314J \cdot mol^{-1} \cdot k^{-1}$).

If the sample temperature is changed by a constant heating rate, $\beta = dT/dt$, the variation in the degree of conversion can be analyzed as a function of temperature, which depends on the time of heating. Therefore, the reaction rate may be written as follows:

$$\frac{d\alpha}{dT} = \frac{A}{E}e^{-\frac{E}{RT}}f(\alpha) \tag{3}$$

Integration of this equation from an initial temperature, T_0, corresponding to a degree of conversion α_0, to the peak temperature, T_P, where $\alpha = \alpha_P$, gives:

$$\int_{\alpha_0}^{\alpha_P} \frac{d\alpha}{f(\alpha)} = \frac{A}{\beta} \int_{T_0}^{T_P} e^{-\frac{E}{RT}} dT \tag{4}$$

When T_0 is low enough, $\alpha_0 = 0$, so there is no reaction between 0 and T_0 ;

$$g(\alpha) = \int_{0}^{\alpha_P} \frac{d\alpha}{f(\alpha)} = \frac{A}{\beta} \int_{0}^{T_P} e^{-\frac{E}{RT}} dT \tag{5}$$

where $g(\alpha)$ is the integral function of conversion, which is either a sigmoidal function or a deceleration function. Different expressions for $g(\alpha)$ and $f(\alpha)$ for the different solid-state mechanisms can be achieved from literatures [25]. The functions were satisfactorily used for the estimation of the reaction solid-state mechanism from non-isothermal TGA experiments.

1.6.1   Kissinger method – Differential method

The Kissinger method has been used in this work to determine the activation energy of solid-state reactions from plots of the logarithm of the heating rate versus the inverse of the temperature at the maximum reaction rate in constant heating rate experiments [26]. The Kissinger method is based on the calculation of the apparent activation energy E_a on the temperature at which the maximum rate of weight loss, T_{max} occurs in the TGA cure at several stages.

The Kissinger equation is

$$\ln\frac{\beta}{T_m^2} = \ln[An(1-X)_m^{-1}] - \left\{\frac{E}{RT_m}\right\} \tag{6}$$

where β is the heating rate, A is the pre-exponential factor, n is the order of the reaction and R is the universal gas constant. A plot of $\ln \beta/T_m^2$ versus $(1/T_m)$ then gives $-E/R$ from the slope of the line.

1.6.2 Flynn-Wall-Ozawa Method – Integral method

This method is based on the representation of the degradation reaction by power law kinetics [43]. This method used the approximation of Doyle to evaluate the integrated form of the rate equation and yields eq. (3) as an approximate solution [27]. The current study supposed supposed that $\ln(1 - 2RT/E)$ tends to be zero for the Doyle approximation obtaining in natural logarithmic form. Assuming E/RT >20, it can be obtained:

$$\log(\beta) = \log\frac{AE}{g(\alpha)R} - 2.135 - \frac{0.4567E}{RT} \tag{7}$$

where $g(\alpha)$ represents the weight loss function. E is obtain from a plot of $\log(\beta)$ versus 1000/T for fixed degrees of conversion and the slope of the line is given by $0.4567E/R$.

1.6.3 Coat-Redfern method

The Coat-Redfern method uses an asymptotic approximation for the resolution of Equation 5 [28]. Based on the Doyle approximation that $\ln(1 - 2RT/E)$ tends to be zero, the logarithmic form could be attained as following:

$$\ln\frac{g(\alpha)}{T^2} = \ln\frac{AR}{\beta E} - \frac{E}{RT} \tag{8}$$

The parameters for the different degradation process $g(\alpha)$ can be achieved from Table 1. The activation energy can be generated from the plot of $\ln(g(\alpha)/T^2)$ versus $1000/T$.

1.6.4   Malek method

The activation energy of a solid-state reaction can be determined from several non-isothermal measurements. If the value of the activation energy is known, the kinetic model of the process can be found in the following way [29, 30]. Malek method defines the function:

$$(\alpha) = \frac{\left(\frac{d\alpha}{dt}\right)}{\beta}\pi(x)T \tag{9}$$

where $z(\alpha) = E/RT$, and $\pi(x)$ is an approximation of the temperature integral which cannot be expressed in a simple analytical form. In this study we used the fourth rational expression of the Senum and Yong [31, 32], which gives errors lower than 10^{-5} for x =20. From Equations (1) and (9) we obtain

$$(\alpha) = f(\alpha)g(\alpha) \tag{10}$$

The master plots corresponding to Equation (10) are shown in Figure 5.

1.7 Thermal decomposition study of poly (phenylene sulfide)

Poly (phenylene sulfide) (PPS) is a semi-crystalline plastic with high thermal durability. It also resists organic solvents, chemical corrosion, and ignition, and it can be easily adapted for processing. The degradation behavior of PPS has been studied by numerous researchers. Montando et al. [33] used pyrolysis-mass (Py-MS) to observe the thermal pyrolysis of PPS with different structures. Christopher et al. [34] analyzed the isothermal kinetics of the PPS and perfluropoly (phenylene sulfide) pyrolysis using thermogravimetric analysis (TGA) at temperatures between 350 and 470°C and evaluated their pyrolysis mechanism by Fourier transform infrared

spectroscopy (FTIR). Thus, Montando et al. [35, 36] used Py-MS to analyze the pyrolysis mechanism and pyrolysates of PPS with different substituted groups. Zongying et al. [37] used FTIR to observe the isothermal cracking of PPS in air and nitrogen between 320 and 400°C.

Among those studies, L.H. Perng [38] revealed the decomposition behavior of PPS in detail by stepwise pyrolysis/gas chromatography/mass spectrometry (stepwise Py-GC/MS). The composition of evolved gases was determined by Py-GC/MS analysis. He found that the decomposition process of PPS is one-stage pyrolysis, mainly by depolymerization, main chain random scission and carbonization. The initial scission of PPS is depolymerization and main chain random scission to evolve benzenbethiol and hydrogen sulfide, respectively, as major products. Depolymerization dominated in lower temperature pyrolysis and main chain random scission dominated in higher temperature pyrolysis. The chain transfer of carbonization was also produced in initial pyrolysis and gradually dominated at the higher pyrolysis temperature to form the high char yield of solid residue.

The major evolution profiles of benzenethiol, hydrogen sulfide, benzene and carbon disulfide as a function of peak temperatures are shown in Fig. 1(a). Hydrogen sulfide was always the dominating pyrolysate in the pyrolysis sequence. The formation curve of hydrogen sulfide started to evolve after 550°C and reached maximum around 750°C, indicating the contribution of main chain random scission of the sulfide groups as the major path in the pyrolysis process. The monomer benzenethiol was the next abundant species. It started to form at 550°C, reached maximum between 700 and 750°C and then drastically reduced after 850°C, indicating that depolymerization was also one of the

major pyrolysis paths. More detailed information of pyrolysates' formation could be obtained. In comparison with hydrogen sulfide, benzene formed the same trend with the maximum at 750°C as a result of main chain random scission. The formation of carbon disulfide indicated the contribution to the scission of the incompletely carbonized solid residue after 850°C. This implied that the chain transfer of carbonization increased gradually to become the dominating mechanism in the transition from the lower to higher pyrolysis temperature.

Fig. 1. (a) Change of PPS pyrolysis products in stepwise Py-GC/MS: (1) benzenethiol; (2) hydrogen sulfide; (3) benzene; (4) CS2; (b) Change of PPS pyrolysis products in stepwise Py-GC/MS: (1) diphenyl sulfide; (2) 1,4-benzenethiol; (3) 4-methylbenzenethiol; (4) 4-(phenylthio)-diphenyl sulfide; (c) change of PPS pyrolysis products in stepwise Py-GC/MS: (1) biphenyl; (2) biphenylthiol; (3) 4-(phenyl)-diphenyl sulfide; (d) Change of PPS pyrolysis products in stepwise Py-GC/MS: (1) dibenzothiophene; (2) 4-thiodiphenylsulide; (3) 3-thiodibenzothiophene; (4) 2-(phenylthio)-diben- zothiophene [38].

The evolution profile of diphenyl sulfide, 1,4-benzenedi- thiol, 4-methylbenzenedithiol and 4-(phenylthio)-diphenyl- sulfide as a function of peak temperatures is shown in Fig. 1(b), The first three were similar to that of benzenethiol. The last one started to form at 450°C and reached the same maximum as that of benzenethiol, but it still evolved significantly after 950°C. 4-(Phenylthio)-diphenyl- sulfide was the only pyrolysate produced at the initial flash pyrolysis temperature. This result indicated that it was produced by selective scission at chain ends and chain branches. This local instability at chain ends and chain branches might explain the thermal instability of PPS at 450°C. Fig. 1(c) shows the evolution profiles of biphenyl-derivative pyrolysates including biphenyl, biphenylthiol and 4-(phenyl)-diphenylsulfide as a function of peak temperatures. These pyrolysates started to evolve around 650°C, reached the maximum amount between 750 and 850°C and decreased rapidly after 950°C. This implied that the higher pyrolysis temperature favored the recombination of free radicals by chain scission to form these products. Fig. 1(d) shows the evolution profiles of pyrolysates with high mass and heterocyclic moieties including dibenzothiophene, 4-thiodiphenylsulfide, 3-thiobibenzithiophene and 2-(phenylthos)-dibenzothiophene as a function of peak temperatures. These dibenzofuran-derivative pyrolysates could form by the cyclization of adjacent radicals in the incompletely carbonized solid residues.

To validate the complicated mixture of ion species from TG/MS, the superior separating and selectivity of Py-GC/MS analysis was used to select specific ion species (m/z) for real time generation curves of pyrolysates in TG/MS. The major ionic fragments of Py-GC/MS in Table 1 were selected for plotting, although diphenylsulfide and biphenylthiol, having the same m/z, could not be resolved.

Fig. 2(a) shows the real-time evolution curves of benzenethiol, hydrogen sulfide, benzene and CS_2 from TG/ MS analysis. Benzenethiol, as the major product, started to evolve around 460°C, reached maximum around 530°C and decreased drastically around 580°C. Similarly, hydrogen sulfide, as another major product, began to evolve about 460°C and reached the maximum amount about 550°C. The evolution curve of hydrogen sulfide was similar to those of benzene and carbon disulfide. Benzenethiol and hydrogen sulfide evolved in the initial pyrolysis stage, indicating that the initial scission of PPS was depolymerization and main chain random scission. Benzenethiol reached the maximum evolution at a lower temperature than hydrogen sulfide, indicating that depolymerization dominated in lower-temperature pyrolysis and main chain random scission dominated in higher-temperature pyrolysis. From comparison of the curves in Figs. 1(a) and 2(a), it can be seen that similar changes happened during pyrolysis, except CS_2 in Py-GC/MS formed at a higher temperature. The evolution pattern of CS_2 resembled that of hydrogen sulfide, indicating that the initial scission of PPS also produced simultaneously the chain transfer of carbonization. In addition, the evolution curves of CS_2 and benzene after 650°C indicate that higher temperature pyrolysis might be the result of scission in the unstable carbonization residue. The evolution curves of 1,4-benzenedithiol, 4-methyl- benzenethiol, diphenylsulfide+biphenylthiol and biphenyl are shown in Fig. 2(b). The temperature for maximum formation was 530°C for 1,4-benzenedithiol and 4-methylbenzenethiol, being similar to that found in stepwise Py-GC/MS as a result of depolymerization. The formation curves of biphenylthiol diphenyl sulfide and biphenyl as products from recombination of free radicals in main chain random

19

scission were similar to that of hydrogen sulfide, reaching the maxima around 550 and 560°C, respectively. The result resembled that in stepwise Py-GC/MS. The evolution curves of 4-thiodiphenyl sulfide and dibenzothiophene are shown in Fig. 2(c). The maximum formation for dibenzothiophene was about 590°C, indicating cyclization of adjacent radicals in high temperature environment. 4-Thiodiphenylsulfide reached the maximum formation about 550°C and decreased significantly until after 650°C, resembling the results of Fig. 2(d). Hence, the results indicate that the dibenzothiophene had more probability to evolve along with the main chain random scission than the depolymerization.
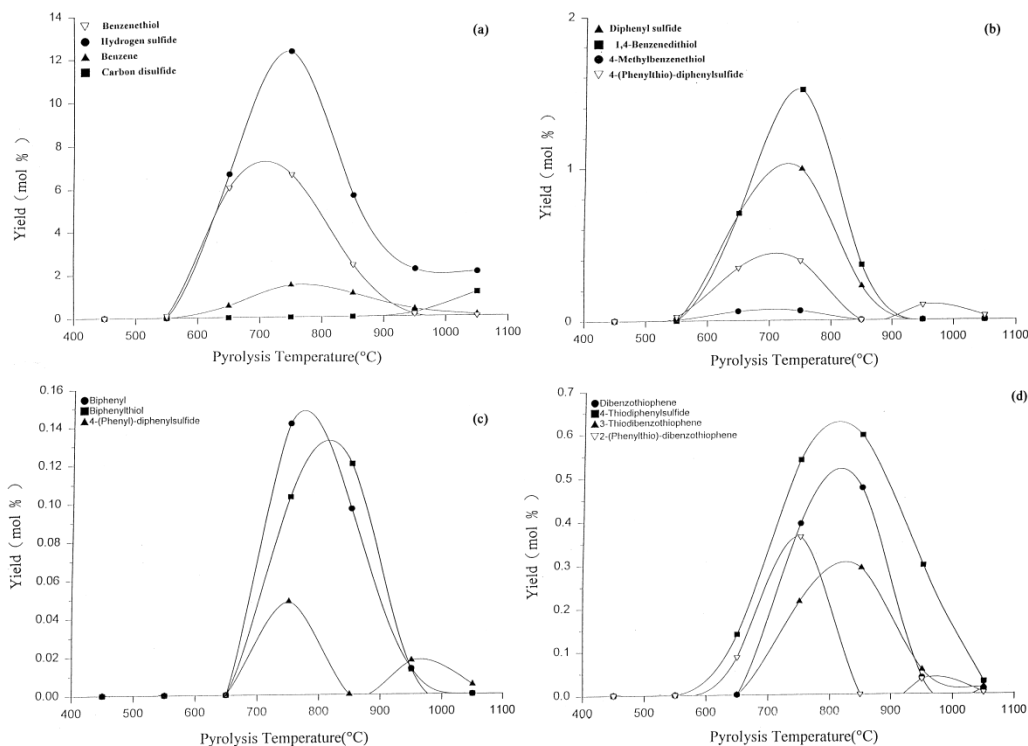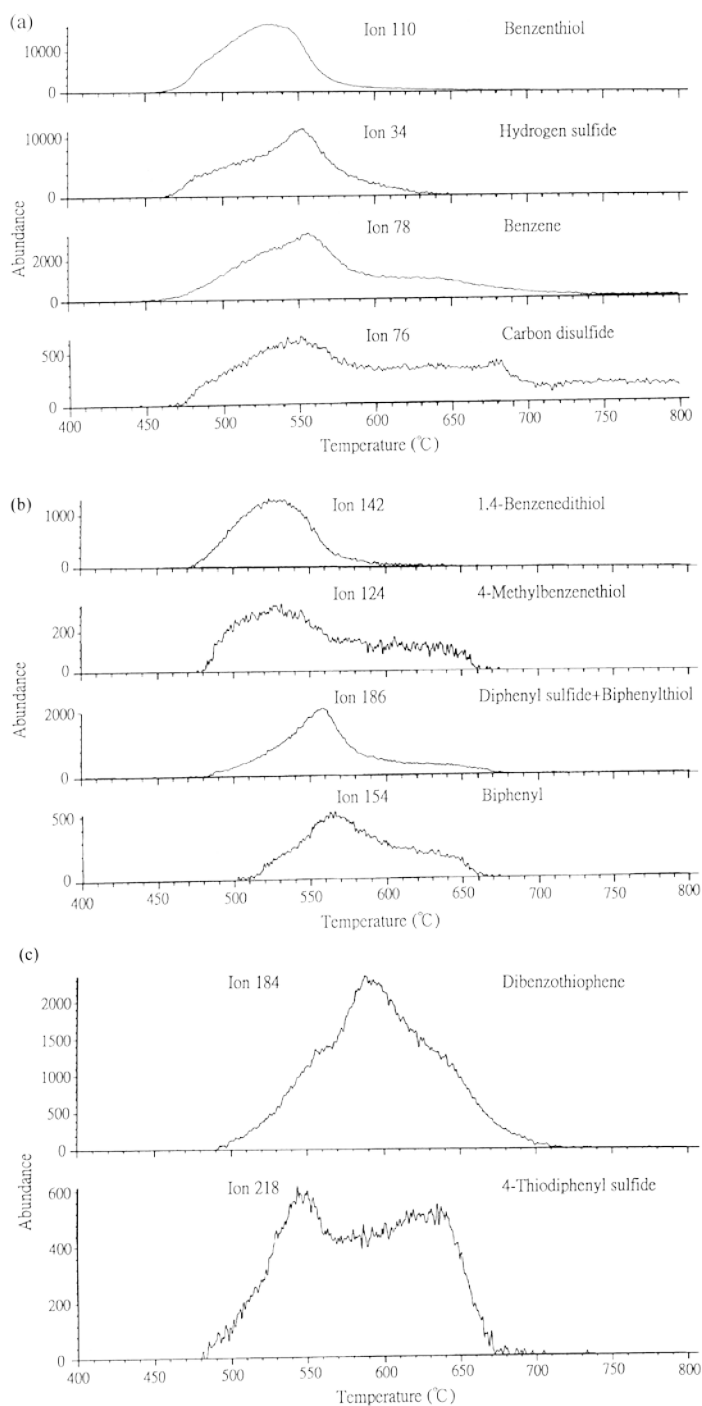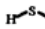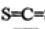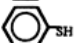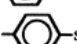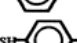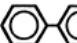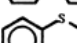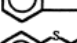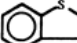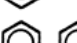
Fig.2. (a) Change of PPS pyrolysis products in TG/MS in He at 10 °C /min: (1)
benzenethiol; (2) hydrogen sulfide; (3) benzene (4) CS$_2$; (b) change of PPS pyrolysis
products in TG/MS in He at 10 °C /min: (1) 1,4-benzenedithiol; (2) 4-
methylbenzenethiol; (3) diphenyl sulfide+biphenylthiol; (4) biphenyl; (c) change of
PPS pyrolysis products in TG/ MS in He at 10 °C /min: (1) dibenzothiophene (2) 4-
thiodiphenylsulfide[38].

Table 1. Identification of products in flash Py-GC/MS of PPS up to 850 °C in He [38].

	Compound	Retention time (min)	Molecular weight	Major mass fragments	Extract TGA/MS analysis
	Hydrogen sulfide	2.3	34	34,33	34
	Carbon disulfide	2.6	76	76,44	76
	Benzene	3.3	78	78,52,51,50,77	78
	Benzenethiol	7.2	110	110,66,109,84,77	110
	4-Methlybenzenethiol	8.9	124	124,91,123	124
	1,4-Benzenedithiol	12.1	142	142,78,109,97	142
	Biphenyl	13.4	154	154,153,152,76,155,51	154
	Diphenyl sulfide	16.0	186	186,185,51,77,171,152	186
	Biphenylthiol	17.5	186	186,185,152,184	186
	Dibenzothiophene	17.9	184	184,139,92,152,183	184
	4-Thiodiphenylsulfide	19.7	218	218,185,184,109	218
	3-Thiodibenzothiophene	21.5	216	216,184,171,139,108	216
	4-(Phenyl)-diphenylsulfide	24.1	262	262,261,263,152,184	262
	4-(Phenylthio)-diphenylsulfide	26.5	294	294,185,184,295	294
	2-(Phenylthio)-dibenzothiophene	29.8	292	292,291,293,290,258	292

1.8 Objectives

Objective 1

Develop a carbonization-in-nitrogen method for measuring the fiber content of carbon fiber reinforced thermoset composites. Study the accuracy of the method by comparing the nominal and experimental results using different resin systems. Verify the consistency and repeatability of the method by applying it to different carbon fiber contents, at different facilities, and by different operators.

Objective 2

Extend the carbonization-in-nitrogen method to carbon fiber reinforced thermoplastic composites and validate the accuracy on the high temperature thermoplastics resins by comparing the nominal carbon fiber content with the experimental results from the carbonization-in-nitrogen method.

Objective 3

Generate the thermal degradation model of the carbon fiber reinforced PPS polymers composites. Investigate the thermal degradation kinetics and implement the attained knowledge to predict the thermal degradation of the carbon fiber reinforced PPS polymer composites. Validate the fundamental assumption of the carbonization-in-nitrogen method: the carbonization of the reference neat resin and the resin in the composites possess same carbonization behavior and same carbonization temperature range (above 535°C).

2. EXPERIMENT APPROACH

2.1 Manufacture of samples

In order to verify the carbonization-in-nitrogen procedure on the thermoset and thermoplastic systems, different carbon fiber contents with different resin composites were prepared by different processing techniques. Thermoset samples were prepared for the epoxy and vinyl ester systems using the hand lay-up process. Thermoplastic samples were prepared by the hot melt impregnation process for PP, PA66, and PPS. The reason to choose the hand lay-up and hot melt impregnation methods is that both of these processes could help us to accurately control the carbon fiber content in the composite sample. Knowing the nominal carbon fiber content in the composite samples is crucial in validating the CIN method in the following study.

2.1.1 Materials

Different kinds of thermosets and thermoplastic resins were used in this research to prepare testing samples. The general information for those systems is described as follows:

Vinyl ester resins (VER) were first introduced in the early 1960s [38]. They combine the advantage of a robust epoxy chain backbone with the reactivity of unsaturated polyester (UP) resins. They also fall in the middle of the price-to-performance ratio of UP resins and epoxy; i.e. they have better property performance when compared to UP resins, while not being as expensive as epoxy resins. Some of advantages of the VER include: no susceptibility to chemical attacks, excellent corrosion and chemical resistance, and good compatibility by good wetting and bonding to fillers and fiber reinforcements for composite applications.

Epoxy resins account for about 4-6% of the total consumption of thermoset in industrialized countries. [39] It is the resin that is predominantly used in most high-end composite applications like aircraft fuselages, wind turbine blades etc. Advantages of epoxies include good mechanical properties, broad range of moduli, good thermal resistance, resistance to numerous organic solvents and chemicals, good electrical properties, strong adhesion properties on a variety of substrates, good flame retardancy properties, and capacity for use in manufacture of high performance composites. Some of their disadvantages are long and energy-expensive production cycles due to low reaction rates, relatively high prices, and health and safety considerations during manufacture.

Thermoplastic composites are typically comprised of a matrix, such as polypropylene (PP), Polyamide66 (PA66), poly phenylene sulfide (PPS), or poly ether ether ketone (PEEK), reinforced with fibers.

PP is a kind of polymer which can be made by polymerizing propylene molecules. It is widely used in many different applications including automotive components, reusable containers of different types, plastic parts, packaging and labeling, loudspeakers and thermal underwear. PP is resistant to different chemical solvents, acids and bases. PP is also very suitable for filling, reinforcing and blending. PP combined with natural-fibrous polymers is one of the most promising routes to create natural-synthetic polymer composites [40].

PPS is a semi-crystalline polymer composed of phenyl rings and sulfur atoms that possesses outstanding mechanical and thermal properties. Composite structures made of PPS remain hard, stiff, and dimensionally stable even when exposed to temperature of

more than 100°C. They resistant to aggressive media; possess inherent flame retardancy, have minimum water absorption, and excellent friction properties [41]. The most important application areas are the automobile, aeronautic, and electronic industries. Carbon fiber reinforced PPS is mainly used in aircraft structural applications, such as in the "J-Nose" wing substructures of the Airbus A340-500/600 [42].

PA66 is a macromolecule with repeating units linked by amide bonds. It is the most important polymer used in many products: insulation foams, elastomers, adhesives, automobiles, appliances, etc. [43, 44]. The utilities of PA66 rest upon its combination of properties and upon its susceptibility to modification. Key properties are good resistance to oils and solvents, high toughness, high fatigue and abrasion resistance, low friction and creep, good stability at elevated temperatures, good fire resistance, good appearance and good processability. Water absorption is the drawback of PA66. PA66-based composites can be found in many applications. Transportation is the largest market for PA66-based composites, as it could be used in the wire jackets, windshield wipers, and speedometer gears. Electrical and electronic applications comprise a major market for PA66.

In this research, the epoxy resin used for all samples was West System Epoxy 105. The curing agent used was West System 206. The resin/curing agent mass ratio was 100/20.5. The vinyl ester resin used was Derakane TM 411-350, manufactured by Ashland. The curing agent was a mixture of the catalyst Trigonox 239, the accelerator Cobalt, and the inhibitor Acetyl Acetone. The resin/curing agent mass ratio was 100/1.95. The carbon fiber fabric sheets were Pyrofil in 12k tows with standard sizing, manufactured by Mitsubishi Rayon Japan.

2.1.2 Manufacture

The thermoset composite samples were processed by hand lay-up. Carbon fiber sheets were cut to 40 mm x 40 mm and weighed to calculate the nominal carbon fiber content in the samples. During the hand lay-up process, a release agent was sprayed on the work surface to form a release layer between the sample and the work surface. The carbon fiber sheet of known weight was placed on the top of a glass table, and then thermoset resin was used to wet out the carbon fiber sheet. A vacuum was applied to create even pressure and draw the trapped air and extra resin for consolidation of the composites. The vinyl ester and epoxy resin samples were cured at room temperature and used for the following carbonization procedure. Figure 3 shows the samples and the hand lay-up process used to prepare the samples.

| (a) | (b) | (c) |
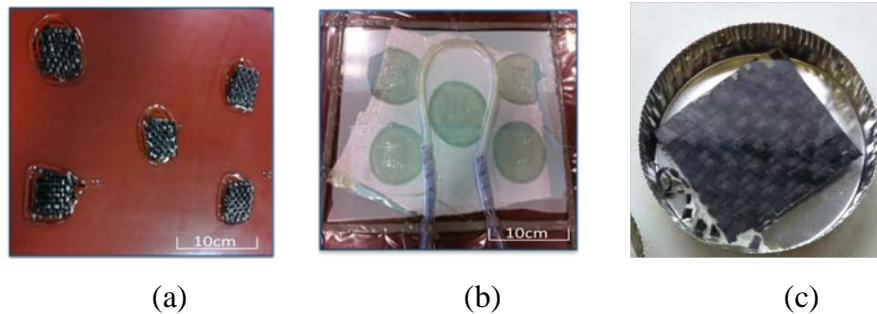
Figure 3. The hand lay-up method to prepare carbon fiber thermoset composite samples. (a) Carbon fiber wet out with resin; (b) vacuum applied to consolidate the individual samples; (c) A representative cured sample with known fiber content ready for carbonization-in-nitrogen testing.

A number of carbon-fiber-reinforced thermoplastic samples were prepared by the hot melt impregnation process in this research. The configuration of the hot melt impregnation is demonstrated in Figure 4. It consists of an extruder, a puller, several hot compactors, and fiber creels. During the preparation, the fiber tow was pulled from a creel and heated above melt temperature. A single extruder compounds the resin. The heated roving was impregnated in the impregnator die with the melted resin by opening

27

the fiber bundles over specially designed pins. The impregnated fiber tow then passed through a series of hot scrapers which scraped excess polymer off of the tow to produce an impregnated tape. After pulling out by the puller, the carbon fiber thermoplastic material was shaped to tapes and then cut into one-inch-long pellets for the following test procedure. Different temperatures were set up for the rollers, impregnator dies and extruders. Table 2 lists the temperature of different sections during the sample processing procedure. In preparing the carbon fiber reinforced PA66 process, the impregnator die temperature was set up at 285°C, and the extrusion zones were set up to 220, 245, and 260°C, respectively. Molten resin was extruded to the die by the single screw to impregnate the fiber. The puller was set up to 4 rpm (revolution per minute) to pull the tape out of the die. Figure 5 shows the extruder in which the raw polymers were fed into the hopper and then heated up above melting temperature.

Table 2 .Materials manufactures information.

Materials	Density (g/cm^3)	Glass Transaction Temperature (°C)	Melting Temperature (°C)
Carbon Fiber	1.75	--	--
PP	0.91	18	165
PA66	1.14	85	265
PPS	1.35	90	285

1：polymer supply;2: extruder;3: impregnator (heating die);
4: preheating rollers;5: fiber creels;6: hot compactors;7: puller

Figure 4. The configuration of the hot melt impregnation line.
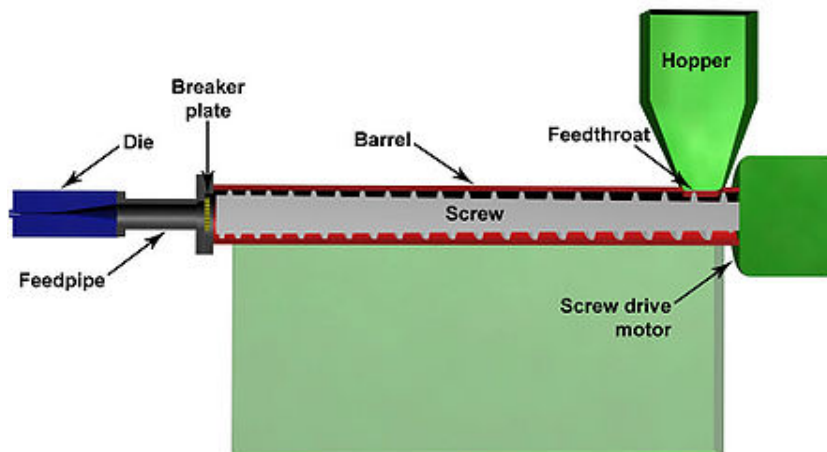
Figure 5. The configuration of the extruder.

2.2 Characterization

2.2.1 DSC and TGA testing

Dynamic Scanning Calorimetery (DSC) Q 100 DSC (TA Insrumetns INC, Delaware) was

used to detect the glass transition temperature of the polymers and samples involved in

this research. The temperature was ramped from ambient temperature to 200°C at the heating rate of 10°C/min^{-1}.

A Thermogravimetric Analyzer (TGA 2950, TA Instrument Inc, Delaware) was used to characterize the thermal degradation and melting temperature of the samples in this research.   The samples in the TGA were heated up to 900°C from the ambient temperature at the heating rate of 5, 10, 20, 40°C/min^{-1} under an air or nitrogen atmosphere.

2.2.2 Sample mass measurement

The sample weight was measured using the balance (Mettler Delta range AT 261) after the sample was dried in an air circulation furnace for at least 12 hours at 60°C. The furnace used was Lindberg Blue M 55367.

2.2.3 Carbonization-in-nitrogen procedure

The carbonization-in-nitrogen method is described in the following procedure: Composite samples and *reference neat resin* samples were placed in a nitrogen-purging tube furnace as shown in Figure 6 after drying. The samples were heated to at least 400°C and held at that temperature for 60 minutes. The resin in the composite samples and *reference neat resin* samples was carbonized simultaneously under identical thermal conditions. The sample residue was weighed after being cooled down to room temperature. Some samples were processed and carbonized at Toray Carbon Fibers America, Decatur, Alabama to prove that the developed method is applicable in different labs. Figure 6(a) shows the residue from the composite sample after carbonization. Figure 6(b) shows the residue from the carbonized *reference neat resin* sample, which is used to

calibrate the percentage of matrix residue from the carbon fiber composite sample as shown in Figure 6(a).
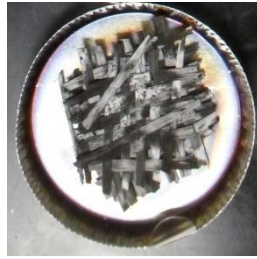
(a)   (b)

Figure 6. (a) Residue after carbonization-in-nitrogen for the sample shown in Figure 5(a); and (b) residue from reference neat resin after carbonization-in-nitrogen for calibration.

3. ORGANIZATION OF WORK

The work has been divided into three manuscripts consistent with the objectives described. Each manuscript builds from the other and is consistent with the objectives for the entire study.

Manuscript 1 describes the carbonization-in-nitrogen procedure. Two kinds of carbon-fiber-reinforced thermoset systems have been prepared and used to validate the new procedure by comparing the nominal results with the experimental results. The results from the carbonization-in-nitrogen method demonstrate that the method can be used as a generalized way to determine fiber content in carbon-fiber-reinforced thermoset composites effectively and accurately.

Manuscript 2 reports the results for the carbon fiber content from the carbonization-in-nitrogen method for three kinds of thermoplastic resin composites. The low deviations

31

between the nominal and experimental results of different fiber content ranges for different thermoplastic systems indicate the carbonization-in-nitrogen method could be extended to thermoplastic resin.

Manuscript 3 reports the thermal degradation behavior on the carbon-fiber-reinforced PPS composites that is used in Manuscript 2. The determination of the kinetic parameters and the degradation mechanism using TGA experiments have been studied to explain CPPS thermal degradation in air or nitrogen based on the activation energy calculation. The thermal degradation mechanism for carbon fiber reinforced poly (phenylene sulfide) (CPPS) is a deceleration (D_n) type, which is a solid-stage process based on an n-dimensional diffusion both in air and nitrogen atmospheres. The degradation behavior of CPPS in the nitrogen atmosphere is a single-stage process, and the activation energy is around 189kJ mol^{-1}. Whilst in the air, it is a two-stage thermal degradation process, where the activation energy for the first step is 202 kJ mol^{-1} and 165 kJ mol^{-1} for the second step. The oxygen stabilizes and promotes random scission benefits. The carbonization behavior of the CPPS and pure PPS are identical above 535°C.

DEVELOPMENT OF A CARBONIZATION-IN-NITROGEN METHOD FOR
MEASURING THE FIBER CONTENT OF CARBON FIBER REINFORCED
THERMOSET COMPOSITES

by

QIUSHI WANG
HAIBIN NING
UDAY VAIDYA
SELVUM PILLAY
LEIGH-ANN NOLEN

33

DEVELOPMENT OF A CARBONIZATION-IN-NITROGEN METHOD FOR MEASURING THE FIBER CONTENT OF CARBON FIBER REINFORCED THERMOSET COMPOSITES

Abstract

Carbon fiber reinforced thermoset composites such as carbon fiber epoxy composites are widely used in aircraft and aerospace, and are being increasingly used in automotive applications because of their lightweight characteristics, high specific strength, and stiffness. The carbon fiber content in the composite plays a critical role in enhancing structural performance. The carbon fibers contribute to the strength and stiffness; therefore, the mechanical properties of the composite are greatly influenced by the carbon fiber content. Measurement of carbon fiber content is essential for product quality control and process optimization. In this work, a novel carbonization-in-nitrogen method is developed to characterize the fiber content in carbon fiber thermoset composites. A carbon fiber composite sample is carbonized in a nitrogen environment at elevated temperatures, alongside a neat resin sample. The carbon fibers are protected from oxidization while the resin (the neat resin and the resin matrix in the composite sample) is carbonized under nitrogen environment. The neat resin sample is used to calibrate the resin carbonization rate and calculate the amount of the resin matrix in the composite sample. The new method has been validated on several thermoset resin systems, and found to yield accurate estimation of fiber content in carbon fiber thermoset composites.

* Corresponding author, Tel.: 205-996-7390; fax: 205-934-8485. Email: ning@uab.edu

Introduction

Carbon fiber reinforced thermoset composites have been widely used in many high-performance applications because of their widely described advantages, especially high specific strength, stiffness and stiffness-to-weight ratios, and many other advantages [1-4]. It is known that the carbon fiber content, as one of the most important parameters, determines the mechanical and other properties of carbon fiber composites. Smith et al (2007), Chen et al (1999) and Simon (1987) et al have studied the effect of fiber content on resulting properties of composite materials [5-7]. Carbon fibers act as the primary reinforcement to provide strength and stiffness for fiber reinforced composites.

Traditionally, standard methods established by ASTM D3171-Standard Test Methods for Constituent Content of Composite Materials are applied for determining fiber content in carbon fiber composites [8]. These methods require that the resin matrix be completely removed from a carbon fiber composite either by acid digestion or burn-off in air and only the carbon fibers remain in the residue. Despite widespread use, the acid digestion and burn-off-in-air methods are not without limitations. The acid digestion method has been restricted to certain resin systems, such as polypropylene and epoxy, which could be dissolved completely in acids. Highly hazardous acids such as hydrochloric and sulfuric acids used in the acid digestion method could pose potential hazards to the operator, as well as the environment. In addition to the excessive time required for acid digestion, there are several semi-crystalline resins (e.g. polyimide) that cannot be dissolved in solvents (e.g. hydrochloric acids) [9]. The burn-off-in-air method is only applicable for resins that are easy to degrade at elevated temperatures. High temperature resins, such as epoxy (decomposition temperature > 400°C) typically used in aircraft and automobile

35

applications, will only totally degrade in air at temperatures that will also cause the carbon fibers to oxidize [10]. In addition, airborne carbon particles from matrix burn-off in air pose potential hazards to the operator and the environment.

Another method used for measuring carbon fiber content is Thermogravimetric Analysis (TGA), as reported by Polis [11]. In this method, a sample weighing less than 0.1 gram is used. This small sample size is not sufficiently representative of carbon fiber composite structures. The TGA method has not been widely adopted because of low confidence level which is derived from using small sample size (0.1 gram) to represent large composite structures.

Optical microscopy is another method which has been reported by Purslow et al (1984) and Cohen et al (2001) [12-13]. The fiber content is measured through optical image analysis, with the image obtained from a polished composite sample. The accuracy of this method is highly dependent on sample preparation, number of cross-sections being examined, and image filtering. In addition, a sufficient number of cross-sectional surfaces should be examined in order to obtain a fiber content representative of the whole sample. This may also lead to misrepresentation of studying three-dimensional features (fiber volume/weight content) using two-dimensional characterization method.

In this paper, a generalized method is developed to measure the carbon fiber content in carbon fiber reinforced thermoset composites.

Experiment

2.1 Procedure Description

A carbonization-in-nitrogen method is developed to characterize carbon fiber reinforced thermoset composites. A carbon fiber reinforced thermoset composite is carbonized in a nitrogen-purging tube furnace along with a *reference neat* (unreinforced) *resin*. The

36

reference neat resin is the same as that used in the carbon fiber reinforced composite. However, it may be difficult to procure the neat resin sample in some cases, which could be the drawback of this method. During carbonization in nitrogen, the resin matrix in the carbon fiber composite and the *reference neat resin* are carbonized under high temperature (400-600°C) and inert atmosphere. The inert atmosphere is required to avoid oxidation of the carbon fibers. The products of the carbonization of the neat resin and the resin from the composite include both gaseous fumes that are vented and carbonized residue that remains in the furnace. The carbonized residue from the *reference neat resin* provides the percentage of carbonization of the resin. This residue information can be used to calculate the amount of resin matrix in the composite. Figure 1 illustrates the procedure. Carbonization rate (CR) of the neat resin can be estimated from the neat resin sample (m) and its residue ($m_{cr} - m_c$) in accordance with Eq. (1):

$$CR = (m_{cr} - m_c) / m \hspace{5cm} (1)$$

where CR - carbonization rate ($0 \leq CR \leq 1$) of the reference neat resin, m_{cr} - residue mass from the reference neat resin sample in its crucible, m_c - the crucible mass and m - reference neat resin sample mass.

The carbon fiber content (in weight percent), W_f, in the composite sample could be calculated in accordance with Eq. (2) that is developed for the first time:

$$W_f = ((M - M_m)/ M) \times 100 = (((M_{cr} - M_c) - M \times CR)/(M \times (1 - CR))) \times 100 \hspace{1.5cm} (2)$$

where W_f - carbon fiber content, M - carbon composite sample mass, M_m - the mass of the resin matrix in the composite sample, M_{cr} - the mass of the composite residue in its crucible, and M_c - the crucible mass.

2.2 Materials and Equipment

In order to verify the procedure described above, experiments were conducted with two typical carbon fiber reinforced thermoset systems – carbon fiber/epoxy and carbon fiber/vinyl ester because they are commonly used resin systems. Samples with known fiber contents were manufactured using hand lay-up process. In addition, some composite samples were tested in Toray Carbon Fibers America, Decatur, AL which followed the same carbonization procedure mentioned above in order to eliminate the variations caused by the operator and equipment. The known carbon fiber contents of these samples were used to compare to the results obtained from the developed carbonization procedure. The materials and equipment, the carbonization procedure, the manufacture and characterization of the composites, and the experimental uncertainties are introduced in the following sections.

The epoxy resin used for all samples was West System Epoxy 105. The curing agent used was West System 206. The resin/curing agent mass ratio was 100/20.5. The vinyl ester resin used was Derakane TM 411-350, manufactured from Ashland. The curing agent is a mixer of catalyst Trigonox 239, accelerator of Cobalt and inhibitor of Acetyl Acetone. The resin/curing agent mass ratio was 100/1.95. The carbon fibers fabric sheets were Pyrofil in 12k tows with standard sizing, manufactured from Mitsubishi Rayon Japan. The furnace used was Lindberg Blue M 55367. The sample mass was measured on a Mettler Delta range AT 261 balance. Thermogravimetric analyses were done on a Dupont TGA 2950 analyzer.

2.3 Determination of Carbonization Temperature

Thermo-gravimetric analysis (TGA) was conducted on constituent resin and carbon fibers to determine an optimized temperature to carbonize the samples in nitrogen. Figure 2 and 3 illustrate the results for the matrix epoxy resin and vinyl ester used in this study, respectively. The heating rate was 20°C/min and each sample was held at 600°C for 120 min. The epoxy and vinyl ester resins have approximately 15% mass loss at around 350°C. The nearly flat line on the TGA curves indicates that there is no noticeable mass change after 100-minute dwell at 600°C. The carbonized residue percentage for epoxy and vinyl ester is 5.0% and 4.1%, respectively. Figure 4 shows an isothermal curve for carbon fiber at 600 °C, it shows a mass loss of around 1.2% mass fraction occurs after 60 minutes. The mass loss is attributed to the sizing degradation and possible moisture. Based on the TGA results, the temperature for the carbonization in nitrogen is determined to range from 400 to 600°C. In this temperature range, carbon fiber shows no degradation while the resin shows relatively stable carbonization rate.

2.4 Sample Manufacturing

A number of composite samples with different carbon fiber contents were prepared for testing at the UAB Materials Processing and Applications Development (MPAD) Center. The samples involved three different compositions (20-30%, 40-50%, 60-70%) based on the number of carbon fabric layers. The composites were processed by hand lay-up. Carbon fiber sheet was cut to 40 mm x 40 mm and weighed to a predetermined mixture depending on the desired composition. During the hand lay-up process, the release agent was sprayed on the work surface to form a release layer between the sample and the work surface. A carbon fiber sheet of known weight was placed on the top of a glass table and then thermoset resin was used to wet out the carbon fiber sheet. A vacuum was applied to

create even pressure, and draw the trapped air and extra resin for consolidation of the composites. The vinyl ester and epoxy resin samples were cured at room temperature and used for the following carbonization procedure. Figure 5 shows the samples and the hand lay-up process used to prepare the samples.

2.5 Carbonization in Nitrogen

The composite samples and the *reference neat resin* samples were placed in a nitrogen-purging tube furnace as shown in Figure 6 after drying. The samples were heated to at least 400°C and held at that temperature for 60 minutes. The resin in the composite samples and *reference neat resin* samples was carbonized simultaneously under identical thermal conditions. The sample residue was weighed after being cooled down to room temperature. Some samples were processed and carbonized at Toray Carbon Fibers America, Decatur, Alabama to prove that the developed method is applicable in different labs. Figure 7(a) shows the residue from the composite sample after carbonization. Figure 7(b) shows the residue from the carbonized *reference neat resin* sample, which is used to calibrate the percentage of matrix residue from the carbon fiber composite sample shown in Figure 7(a).

Results and Discussion

3.1 Carbon Fiber Vinyl Ester Composite

Table 1 illustrates a comparison between the nominal fiber content and the measured fiber contents from carbonization tests for a batch of carbon/vinyl ester samples. The nominal fiber content was obtained by using the mass of dry carbon fiber over the mass of the cured composite sample during the sample preparation process. The carbon fiber content from the carbonization test was calculated from Equation 2. The deviation of the carbon fiber content between the nominal and carbonization-in-nitrogen method is

40

minimal when compared to the nominal fiber content as shown in Figure 8. The small deviation indicates the carbonization-in-nitrogen method could be used to measure the carbon fiber content in the carbon/vinyl ester samples. The small deviation could be attributed to possible moisture absorption and the sizing of the carbon fiber.

3.2 Carbon Fiber Epoxy Composite

Table 2 lists the measured fiber contents for a set of carbon fiber reinforced epoxy samples used in validating the developed method. The deviation between the actual nominal fiber content and the fiber content from developed carbonization-in-nitrogen method is minimal as illustrated in Table 2. It indicates the developed method could be used to calculate the carbon fiber weight fraction in the epoxy resin composites. Figure 9 shows the comparison between the calculated results with the nominal results for carbon/epoxy samples for a batch of 5 samples. The small deviations illustrate that the carbonization-in-nitrogen method could be applied to the epoxy system.

Figure 10 summarizes different batches of samples carbonized at different times, with different carbon fiber contents, at different testing facilities, at different temperatures, and by different operators. The results in Figure 10 show that the calculated carbon fiber contents in epoxy and vinyl ester are similar to the actual nominal fiber contents with no more than 2 wt% deviation. Considering the fiber content is normally over 40 wt%, the deviation is minimal. Sizing degradation is not considered in the calculation because of its negligible effect on the results. The low deviation indicates that this method is suitable in determining the fiber content in practice as a generalized method.

Conclusion

A new carbonization-in-nitrogen method has been developed to measure the fiber content in carbon fiber thermoset matrix composites. A reference neat resin sample was carbonized with a carbon fiber thermoset composite sample under nitrogen environment at a temperature ranging from 400°C to 600°C. The carbon fibers were protected from oxidization while the resin was carbonized. The carbonization rate of the reference neat resin sample was used to calculate the amount of the resin matrix in the composite sample. The results from the carbonization-in-nitrogen method demonstrate that the method can be used as a generalized way to determine fiber content in carbon fiber reinforced thermoset composites effectively and accurately.

Acknowledgements

References

[1] L.A. Dobrzaski, A. Pusz, and A.J. Nowak, Aramid-silicon laminated material with special properties-new perspective of its usage, Journal of Achievements in Materials and Manufacturing Engineering, 28/1 (2008) 7-14.

[2] W. Hufenbach, L.A. Dobrzaski, M. Gude, J. Konieczny, and A.Czulak, Optimization of the rivet joints of the CFRP composite material and aluminum alloy, Journal of Achievements in Materials and Manufacturing Engineering, 20 (2007) 119-122.

[3] K. Jamroziak, and M. Bocian, Identification of composite materials at high speed deformation with the use of degenerated model, Journal of Achievements in Materials and Manufacturing Engineering, 28/2 (2008) 171-174.

[4] S.B. Heru, J. Komotori, M. Shimizu, and Y. Miyano, Effects of the fiber content on the longitudinal tensile fracture behavior of uni-directional carbon/epoxy composites, Journal of Materials Processing Technology, 67 (1997) 89-93.

[5] Okoli, and G.F. Smith, Failure modes of fiber reinforced composites: The effect of strain rate and fiber content, Journal of Materials Science, 33 (1998) 5415-5422.

[6] J.H. Chen, E. Schulz, J. Bohse, G. Hinrichsen, Effect of fiber content on the interlaminar fracture toughness of unidirectional glass-fiber/polyamide composite, Composites A, 30 (1999) 747-755.

[7] S. Simon and L. Strunk, Fibre volume of resin matrix composites by density measurement, Int. SAMPE Symp. Exihib. 32 (1987) 116-22.

[8] ASTM D3171 Test method for constituent content of composite materials. ASTM International, West Conchohocken, 2012

[9] Dupont Kapton Polyimide Film General Specifications, Bulletin GS-96-7, http://www.dupont.com/kapton/general/H-38479-4.pdf , accessed in August 2014.

[10] C.L. Chiang and R.C. Chang. Thermal stability and degradation kinetics of novel organic/inorganic epoxy hybrid containing nitrogen/slicon/phosphorus by sol-gel method, Thermochimica Acta, 453(2007) 97-104.

[11] L. P. Daniel and M.F. Sovinski, Determination of fiber volume in carbon/cyannate ester composites using thermogravimetric analysis (TGA), NASA/TM–2006–214143.

[12] D. Purslow, On the optical assessment of the void content in composite materials, Composites, 15 (1984) 207–210.

[13] D. Cohen, S.C. Mantell, and L. Zhao. The effect of fiber volume fraction on filament wound composite pressure vessel strength, Composites, 32B (2001) 413-429.

Table 1. The fiber content results for one batch of carbon vinyl ester samples.

Sample	Total mass (g)	Carbon Fiber mass (g)	Residue mass (g)	Nominal Fiber Content	Fiber Content from Carbonization in N_2	Deviation
C/VE-1	3.593	2.22	2.404	61.8%	62.1%	**0.3%**
C/VE-2	3.707	2.24	2.424	60.4%	60.4%	**-0.1%**
C/VE-3	3.363	2.15	2.336	63.9%	65.0%	**1.1%**
C/VE-4	2.996	1.90	2.038	63.4%	63.4%	**0.0%**
C/VE-5	3.378	2.06	2.186	61.0%	59.6%	**-1.4%**
Neat VE	2.890	--	0.366	--	--	--

Table 2. The fiber content results for one batch of carbon epoxy samples.

Sample	Total Mass (g)	Carbon Fiber Mass (g)	Residue Mass (g)	Nominal Fiber Content	Fiber Content from Carbonization in N_2	Deviation
C/Epoxy-1	4.505	1.783	1.961	39.6%	39.9%	**0.3%**
C/Epoxy-2	4.095	1.730	1.887	42.2%	42.6%	**0.4%**
C/Epoxy-3	3.977	1.897	2.000	47.7%	47.1%	**-0.6%**
C/Epoxy-4	3.998	1.806	1.956	45.2%	45.6%	**0.5%**
C/Epoxy-5	4.348	1.811	1.954	41.6%	41.4%	**-0.3%**
Neat epoxy	5.667	--	0.343	--	--	--
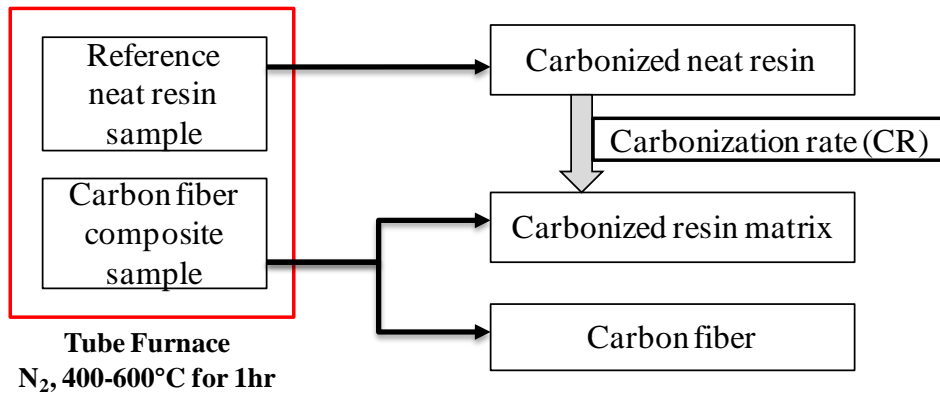
Figure 1. The carbonization-in-nitrogen flow chart. Note that the carbonization rate (CR) is used for calculating the amount of resin matrix in the composite sample.
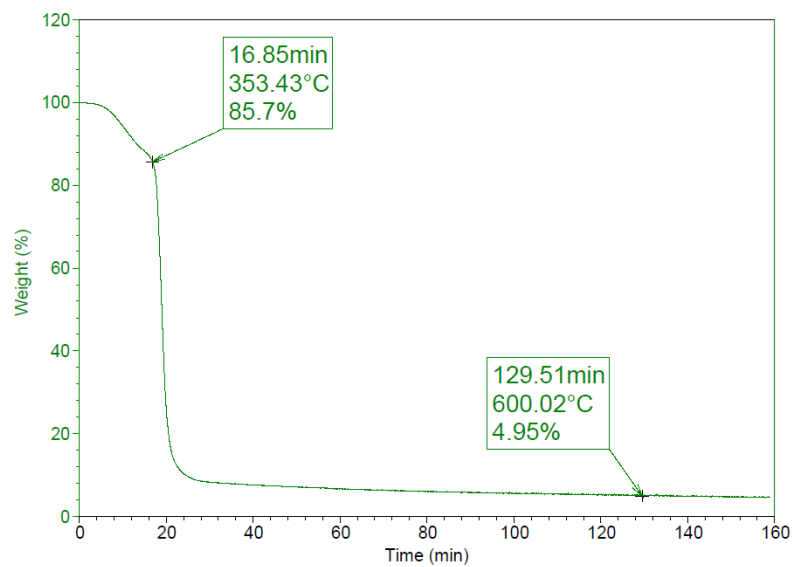
Figure 2. TGA plot of the mass fraction loss of epoxy resin at 600°C. Note that the resin still has residue after 60 min in nitrogen.
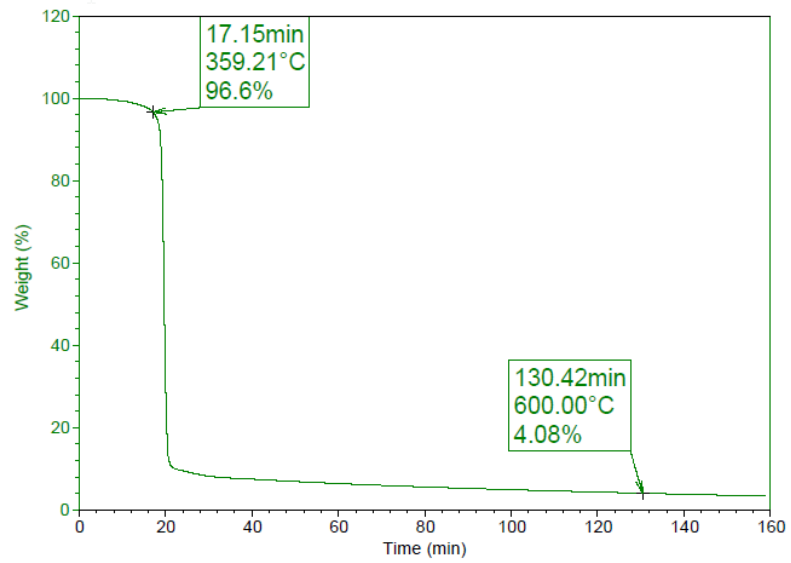
Figure 3. TGA plot of the mass fraction loss of vinyl ester resin at 600°C. Note that the resin still has residue after 60 min in nitrogen.
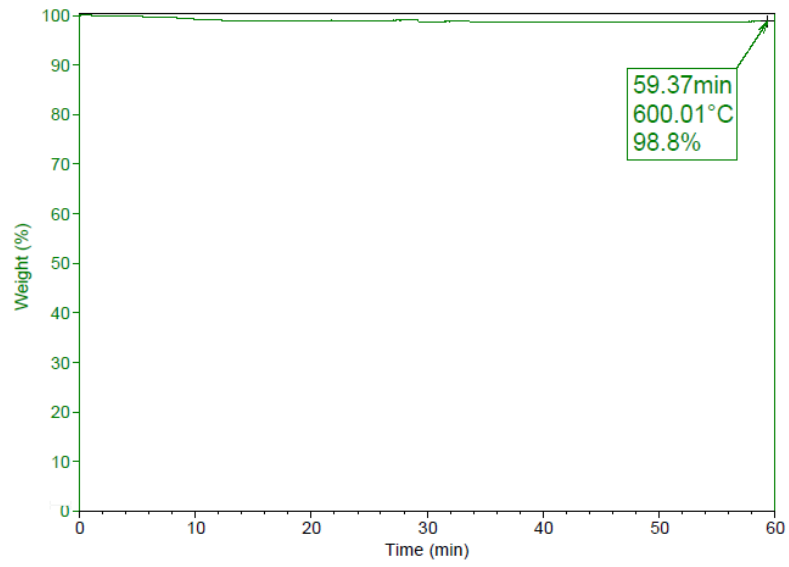
Figure 4. TGA plot of the mass fraction loss of carbon fiber at 600°C in nitrogen.

(a) (b) (c)
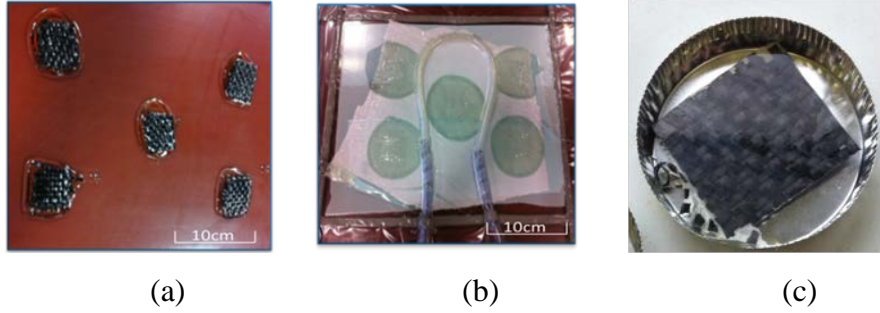
Figure 5. Hand lay-up method to prepare carbon fiber thermoset composite samples. (a) Carbon fiber wet out with resin; (b) vacuum applied to consolidate the individual samples; (c) A representative cured sample with known fiber content ready for carbonization-in-nitrogen testing.
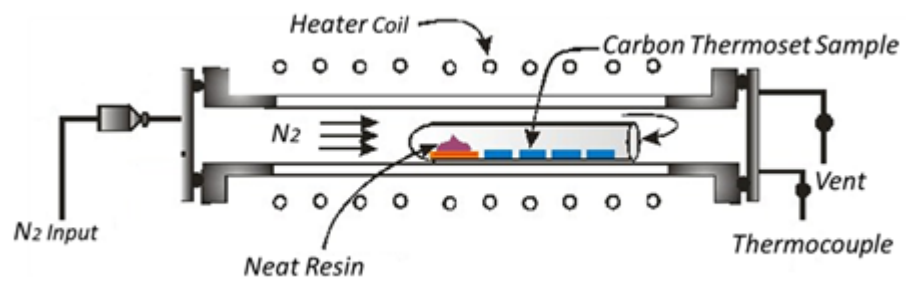
Figure 6. Tube furnace used for the carbonization method.

(a)   (b)

Figure 7. (a) Residue after carbonization-in-nitrogen for the sample shown in Figure 5(c); and (b) residue from reference neat resin after carbonization-in-nitrogen for calibration.
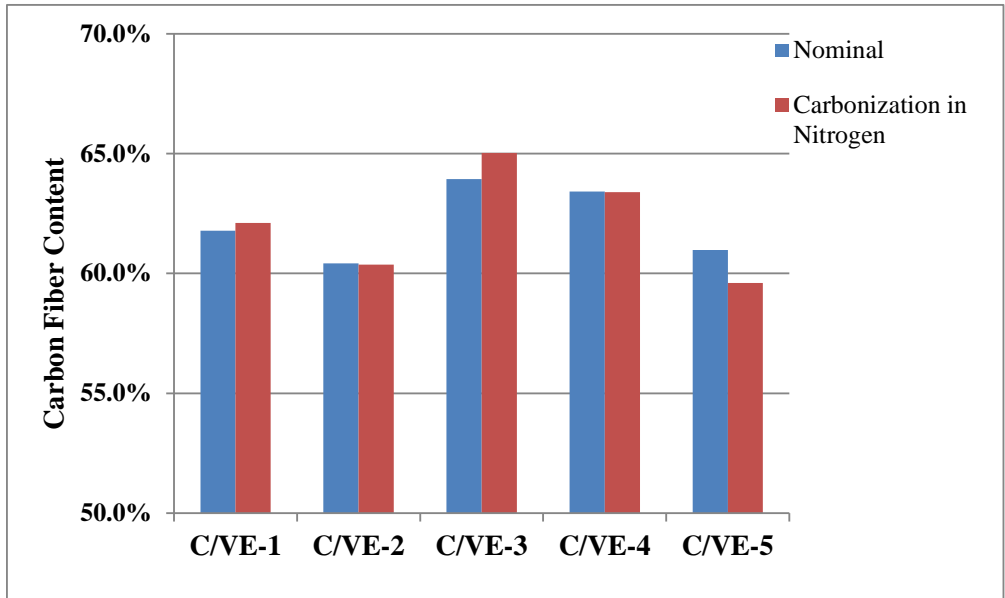
Figure 8. Comparison between fiber content from carbonization in nitrogen and nominal fiber content in a batch of five carbon vinyl ester samples.
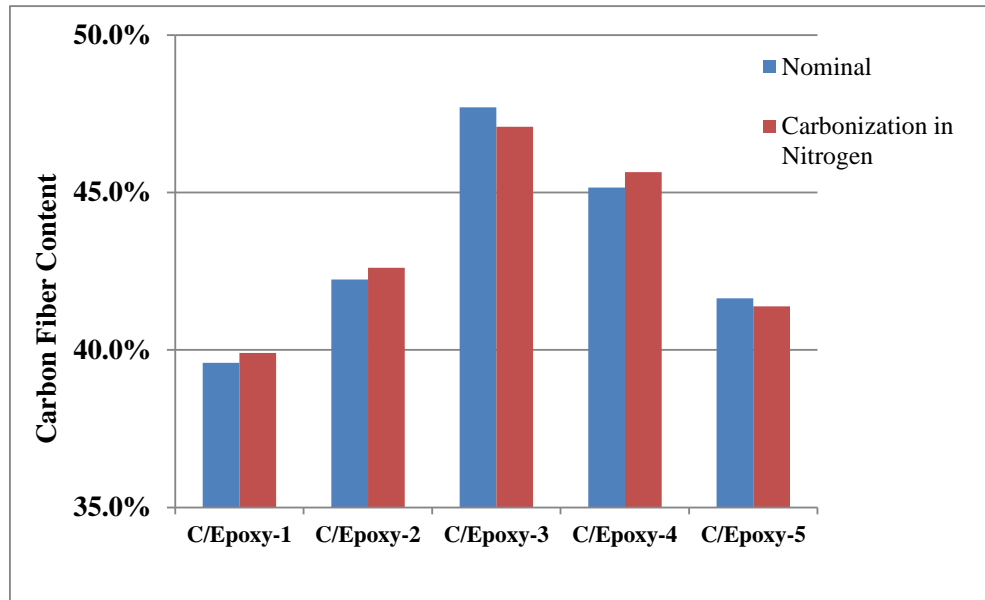
Figure 9. Comparison between fiber content from carbonization in nitrogen and nominal fiber content in a batch of five carbon epoxy samples.
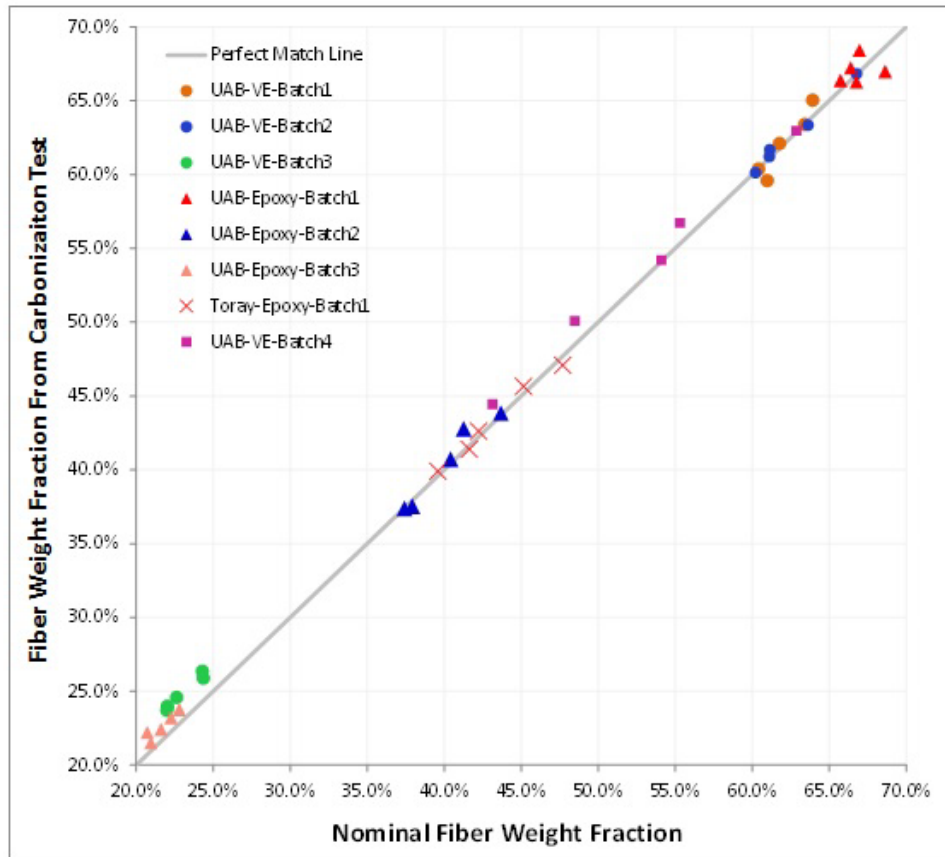
Figure 10. The comparison between the actual fiber content with the fiber content measured using the developed carbonization method.

MEASUREMENT OF THE FIBER CONTENT OF CARBON FIBER REINFORCED
THERMOPLASTIC COMPOSITES USING CARBONIZATION-IN-NITROGEN
METHOD

by

QIUSHI WANG
HAIBIN NING
UDAY VAIDYA
SELVUM PILLAY

MEASUREMENT OF THE FIBER CONTENT OF CARBON FIBER REINFORCED THERMOPLASTIC COMPOSITES USING CARBONIZATION-IN-NITROGEN METHOD

Abstract

Thermoplastic composites are gaining increasing interest in various applications thanks to their combined properties of high specific stiffness, high specific strength, superior toughness, reduction in flammability, good smoke and toxicity performance and insensitivity to chemical attack. Thermoplastic composites with high-modulus carbon fibers have been in use for decades. Their mechanical properties are highly dependent on the carbon fiber content. Fiber content measurement has been difficult using traditional measurement methods for composites with a high temperature thermoplastic matrix such as PPS. In this study the carbonization-in-nitrogen method (CIN) developed in previous work is used to measure carbon fiber reinforced thermoplastic composites and the accuracy of the measurement is verified. In the verification experiment, three kinds of carbon fiber thermoplastic composite samples were prepared by hot melt impregnation method. The carbon fiber thermoplastic composite sample is carbonized in a nitrogen environment alongside a neat resin sample that is used for calibrating the resin carbonization percentage. A good agreement is achieved between the nominal and the experimental carbon fiber content. It is concluded that the carbonization-in-nitrogen method is an accurate and efficient way to characterize the carbon fiber content for carbon fiber thermoplastic composites.

* Corresponding author, Tel.: 205-996-7390; fax: 205-934-8485. Email: ning@uab.edu

Introduction

Thermoplastic composites are attractive for their excellent properties such as high strain to break, indefinite shelf life, ability to thermoform, and light weight, and therefore they have been widely used in many high-performance applications, especially in the aerospace and automobile industries. There are different kinds of reinforcements (glass fiber, carbon fiber, Kevlar, etc.) that have been added into the thermoplastic to suit specific requirements. Although the majority of fiber reinforced thermoplastics contain glass fibers, the attractive properties of carbon fibers (CFs) have made them materials of choice in various applications. CFs have higher stiffness, electrical and thermal conductivity, and resistance to fatigue and creep in comparison to the glass fibers. Carbon fiber reinforced thermoplastics have been manufactured during the last several decades to develop materials that combine high stiffness and strength with low density. The combination of properties has led to a strong increase in the use of these composites for applications in the aeronautic, automotive and energy sectors, replacing traditional materials such as steel, aluminum and wood, amongst others. Thermoplastics offer some advantages over thermosetting resins, namely improved chemical and impact resistance as well as a wider application-temperature range for several high-temperature thermoplastic systems. Moreover, they have a very low level of moisture absorption; hence their mechanical properties are retained under harsh environmental conditions. Another key aspect is shelf life; unlike thermosets, thermoplastic can be easily stored for long periods of time without a loss of performance or the ability to process. These materials with complex shape can be easily manufactured in a few steps through injection, pultrusion and thermoforming process, and offer the possibility to be remelted, providing recycling opportunities [1-4].

A carbonization-in-nitrogen (CIN) method has been developed for measuring the fiber content of carbon fiber thermoset composites in previous work by the authors [5]. A reference neat resin sample was carbonized along with the composites sample with the same resin matrix. The residue from the reference neat resin was used to calibrate the carbonization rate of the resin that was used to calculate the amount of the resin matrix in the composites. The accuracy and repeatability of this method have been verified using thermoset resin systems such as vinyl ester and epoxy resins. In this study, the carbonization-in-nitrogen method (CIN) is used to determine the carbon fiber content of carbon fiber thermoplastic composites. Three kinds of carbon fiber reinforced thermoplastic systems (polypropylene, polyamide66 and poly (phenylene sulfide)) are used and their nominal and experimental fiber contents are compared.

Experiment

Procedure Description

In this study, the previously-developed carbonization-in-nitrogen method was used to determine the carbon fiber content in the carbon fiber thermoplastic composites. This method measures the carbon fiber content by using the carbonization rate of neat resin in the composites and protects the carbon fiber under an inert atmosphere.

Based on the description of the previous work, the carbon fiber content, W_f, in the composite specimen could be calculated in accordance with Eq. (1):

$$W_f = ((M_{cr} - M_c) - M \times CR)/((M \times (1 - CR)) \times 100 \qquad (1)$$

where W_f - carbon fiber content (in weight percent), M - carbon composite sample mass, M_{cr} - the mass of the composite residue in its crucible, M_c - the crucible mass, CR - carbonization rate of the reference neat resin.

Sample Preparation

In order to verify the procedure described above, experiments were conducted on three commonly used carbon fiber reinforced thermoplastic systems: carbon fiber/polypropylene (PP), carbon fiber/polyamide (PA66) and carbon fiber/polyphenylene sulfide (PPS). Samples with a variety of known carbon fiber contents were manufactured by the hot melt impregnation process. In the hot melt impregnation process, the actual carbon fiber content in the composite can be well controlled. The known carbon fiber contents of these samples were used to compare to the results achieved from the CIN method. The materials and equipment, the carbonization procedure, the manufacture and characterization of the composites, and the experimental uncertainties are introduced in the following sections.

Materials and Equipment

Three different kinds of commercially available resins were used in this study to prepare the thermoplastic samples. The Pyrofil X 0327 carbon fiber with a 12 K and 24 K tow size were manufactured from Mitsubishi Rayon Japan. The information of all materials is listed in the Table 1. The furnace which was used to carbonize samples was Lindber Blue M 55367. The mass was measured on a Mettler Delta range AT 261 balance. Thermogravimetric analysis was done on a Dupont TGA 2950 analyzer.

Determination of Carbonization Temperature

Thermo-gravimetric analysis (TGA) was conducted on constituent resin and carbon fibers to determine an optimized temperature to carbonize the samples in nitrogen. Figure 3 illustrates the TGA results for the matrix PP, PA66, and PPS resin used in this study. The

heating rate was 20°C/min and the sample was held at 800°C in nitrogen atmosphere for 120 min for both the resins. The nearly flat line on the TGA curves indicates that there is no noticeable mass change after a 100-minute dwell at 600°C. The carbonized residue percentage of PP, PA66, and PPS is 9.8%, 10.2%, and 35.7%, respectively. The previous research indicates that the carbon fibers will loss its1.5% mass after 60 minutes at 600°C. The mass loss is attributed to the sizing degradation and possible moisture. Based on the TGA results, the temperature for the carbonization in nitrogen is determined to range from 400 to 600°C. In this temperature range, carbon fiber shows no degradation while the resin shows a relatively stable carbonization rate.

Carbonization in Nitrogen

The same heating procedure as described in previous work on the carbonization-in-nitrogen method for thermoset resin was used for this research. The composite samples and the *reference neat resin* samples were placed in a nitrogen-purging tube furnace after drying. The samples were heated to at least 400°C with 10°C/min heating rate and held at that temperature for 60 min. The resin in the composite samples and *reference neat resin* samples were carbonized simultaneously and therefore under identical thermal conditions. The sample residue was weighed after cooling. Figure 4(a) shows the carbon fiber thermoplastic composite sample with known nominal fiber content before carbonization, Figure 4(b) shows residue from that sample after carbonization, and Figure 4(c) shows the residue from the reference neat resin after carbonization. The residue from the reference neat resin was used to calibrate the percentage of matrix residue from the carbon fiber thermoplastic composite sample.

Results and Discussion

Carbon Fiber Contents of Polypropylene Samples

The accuracy of this method has been established by measuring the deviation between the nominal and carbonization test results of the carbon fiber reinforced polypropylene samples. Table 3 illustrates a comparison between the nominal fiber content and measured fiber contents from the carbonization test. The nominal fiber content was obtained by using the mass of one-inch dry carbon fiber over the mass of the one-inch carbon fiber thermoplastic tape. The carbon fiber content from the carbonization test was achieved from Equation 2. The deviation of the carbon fiber content between the nominal and carbonization method is minimal when compared to the nominal fiber content in Figure 5. The small deviation indicates the carbonization method could be used to measure the carbon fiber content in the carbon/polypropylene samples. The small deviation could be attributed to uncertainties in the measurement and the sizing of the carbon fiber.

Carbon Fiber Content of Polyamide Samples

Table 4 lists the measured fiber content for a set of carbon fiber reinforced polyamide samples used in validating the developed method. The deviation between the actual nominal fiber content and the fiber content from the developed carbonization method is minimal compared to the nominal results as illustrated in Table 4. It indicates the developed method could be used to calculate the carbon fiber weight fraction in the polyamide resin composites. Figure 6 shows the comparison between the calculated results with the nominal results in carbon/ polyamide samples for a batch of 5 samples. The small deviations illustrate that the carbonization method could be applied to the polyamide system.

64

Carbon Fiber Content of Polyphenylene sulfide Samples

The comparison of fiber content between the nominal and carbonization tests for a batch of carbon fiber reinforced polyphenylene sulfide (C/PPS) samples are listed in Table 5. PPS is a semicrystalline thermoplastic polymer which does not have any solvent below 200°C [6].The nominal fiber content of the C/PPS was measured by using the mass of five-inch dry carbon fiber over the mass of the five-inch thermoplastic tape from the hot melt impregnation line. The carbon fiber content from the carbonization test was calculated from Equation 2. Figure 7 clearly demonstrates the deviation of carbon fiber content between the nominal and carbonization methods. The largest deviation is 1.4%, which is minimal compared to the nominal fiber content, which is around 40%. The small deviation indicates that the prediction result from the CIN method has a good agreement with the nominal results and could be applied to measure the carbon fiber content in the carbon/polyphenylene sulfide samples. The sizing of the carbon fiber could contribute to the deviation.

Carbon Fiber Content Measurements

The carbon fiber contents of the C/PP and C/PPS were measured by ASTM burn off in air and microscopic methods and compared to the results from the CIN method.

ASTM D3171 determines the fiber content of composites by removing the matrix by digestion or ignition procedures, leaving the reinforcement essentially unaffected and thus allowing the calculation of the reinforcement of matrix content (by weight or volume) as well as the percentage of voids. This methods assumes that the reinforcement is essentially unaffected by the digestion medium. In this research, the burn-off-in-air method was chosen to remove the matrix materials in the composites.

The carbon fiber reinforced PP and PPS composites were heated up to 500°C in the air and held at 500°C for one hour. The fiber content (in weight percent) of the samples could be calculated by the following equation:

$$W_r = M_f / M_i \ x100 \qquad\qquad\qquad (2)$$

where: M_i initial mass of the specimen, g and M_f finial mass of the specimen after burn off, g.

The carbon fiber content results of the C/PP and C/PPS are listed in the Table 6 and Table 7, respectively.

The deviation between the nominal fiber content and content from the ASTM burn off in air is small, as shown in Table 1, which indicates that the ASTM burn off in air method could be used to measure the carbon fiber content in the carbon fiber reinforced PP composites. However, the deviation between the nominal and burn off in air in Table 7 is much larger than in the Table 1, which indicates that the burn off in air could not be used to measure the carbon fiber content in the PPS system at 500°C. The deviation between the nominal and CIN method is minimal compared to the nominal fiber content, shown in Table 5, which indicates that the CIN method is an effective method to evaluate the fiber content in the carbon fiber reinforced PPS composites.

Microscopic methods could also be used to measure the fiber content by analyzing polished slices of the sample. There are two steps involved in this method to measure the carbon fiber content; first measuring the area content of the carbon fiber from the

polished slices and then calculating the carbon fiber mass content by weighting the density of the carbon fiber and matrix PP and PPS polymers.

In this research, the carbon fiber reinforced PP and PPS were cut into slices, polished and characterized with a microscope. Figure 8 shows a typical image of the polished slices of carbon fiber reinforced pp. ImagePro software was used to measure the area fraction of the carbon fiber from the image which is captured with the microscope. Figure 9 shows a typical image of the carbon fiber reinforced PP that has been characterized by the ImagePro method. The white spot in the Figure 9(a) stands for carbon fiber and the dark background is the polymer matrix. The dark circle in the Figure 9(b) was used to capture the carbon fiber diameter and calculated the carbon fiber area content.

The density of the PP and PPS is 1.16 and 1.33 g/cm^3, which are measured by the ASTM D 1505 method. The density of the carbon fiber is $1.75 g/cm^3$ from the manufacture's datasheet.

The carbon fiber contents of the carbon fiber PP and PPS could be calculated by combining the area fraction and density information. Table 8 lists the carbon fiber content results calculated from the microscopic method. The deviation between the nominal and the microscopic method seems larger than the deviation between the nominal and the CIN method. The bigger deviation indicates that the microscopic method could not accurately determine the carbon fiber content in the composites, due to the variations of the density measurement, the area fraction measurement, and the number of the polished slices.

Conclusion

The accuracy and reliability of the carbonization-in-nitrogen method for measuring the carbon fiber content in the thermoplastics resin systems were studied. A reference neat resin sample was carbonized with a carbon fiber thermoplastic composite sample under nitrogen environment at a temperature ranging from 400°C to 600°C. The carbon fibers were protected from oxidization while the resin was carbonized. The carbonization rate of the reference neat resin sample was used to calculate the amount of the resin matrix in the composite sample. The merits of this method could be further amplified when applying it to the high-temperature-resistant and solvent-resistant semi-crystallization PPS resin system. The low deviations between nominal and experimental fiber contents for different thermoplastic systems indicate that the CIN method could be extended to measure the fiber content of carbon fiber thermoplastic composites. The CIN method could measure the carbon fiber content more accurately compared to the ASTM burn off in air method and microscopic method.

Acknowledgements

References

[1] Jiri George Drobny, Applications of Thermal Elastomers. Handbook of Thermoplastic Elastomers, Second Edition, 2014, P301-337

[2] Manson JAE, Walkman MD, Bernet N. Composite processing and manufacturing-an overview. In: Comprehensive composite materials. Oxford, UK: Elsevier Science Ltd.; 200.p.577-607.

[3] Ning H, Vaidya U, Janowski GM, Husman G. Design, manufacture and analysis of a thermoplastic composites frame structure for mass transit. Composite Structure 2007; 80(1) 105-16.

[4] Diaz J, Rubio L. Developments to manufacture structural aeronautical parts in carbon fiber reinforced thermoplastic materials. J Mater Process Technol 2003; 143-144:342-6.

[5] Wang Q, Ning H, Vaidya U. Development of a carbonization-in-nitrogen method for measuring the fiber content of carbon fiber reinforced thermoset composites. Composites Part A, doi:10.1016/j.compositesa.2015.02.025

[6] Diaz J, Rubio L. Developments to manufacture structural aeronautical parts in carbon fiber reinforced thermoplastic materials. J Mater Process Technol 2003; (342-6):143-144.

Tables

Table 1. Materials manufacturer's information.

Materials	Density (g/cm^3)	Glass Transaction Temperature(T_g) (°C)	Melting Temperature(T_m) (°C)
Carbon Fiber	1.75	--	--
PP	0.91	18	165
PA66	1.14	85	265
PPS	1.35	90	285

Table 2. Processing temperature set up for the hot melt impregnation line.

Materials	Melting Temperature (°C)	Extruder Temperature (°C)			Impregnation Die (°C)
		Zone 1	Zone 2	Zone 3 (Hot roller)	
PP	165	130	150	160	200
PA66	265	220	245	260	285
PPS	285	240	260	275	305

Table 3. The fiber content results for one batch of carbon fiber PP samples.

Sample	Total mass (g)	Carbon Fiber mass (g)	Residue mass (g)	Nominal Fiber Content	Fiber Content from Carbonization in N_2	Deviation
C/PP-1	4.0529	0.7752	1.1192	19.1%	19.5%	0.4%
C/PP-2	4.2342	0.7857	1.1421	18.6%	18.8%	0.2%
C/PP-3	3.9864	0.7512	1.0832	18.8%	19.0%	0.2%
C/PP-4	4.2231	0.7869	1.1454	18.6%	18.9%	0.3%
C/PP-5	4.1732	0.7612	1.1087	18.2%	18.3%	0.1%
Neat PP	4.4356	--	0.4476	--	--	--

Table 4. The fiber content results for one batch of carbon fiber PA samples.

Sample	Total mass (g)	Carbon Fiber mass (g)	Residual mass (g)	Nominal Fiber Content	Fiber Content from Carbonization in N_2	Deviation
C/PA66-1	4.0342	0.7223	1.0732	17.9%	17.6%	-0.3%
C/PA66-2	4.2521	0.7168	1.0987	16.9%	16.8%	-0.1%
C/PA66-3	3.8978	0.7114	1.0423	18.3%	17.8%	-0.5%
C/PA66-4	4.1342	0.7823	1.1178	18.9%	18.1%	-0.8%
C/PA66-5	3.9143	0.7234	1.0498	18.5%	17.9%	-0.6%
Neat PA66	3.7933	--	0.4134	--	--	--

Table 5. The fiber content results for one batch of carbon fiber PPS samples.

Sample	Total mass (g)	Carbon Fiber mass (g)	Residue mass (g)	Nominal Fiber Content	Fiber Content from Carbonization in N_2	Deviation
C/PPS-1	5.0324	2.0192	4.1294	40.1%	40.9%	0.8%
C/PPS-2	4.8976	1.9790	4.0320	40.4%	41.8%	1.4%
C/PPS-3	5.1043	2.0217	4.1695	39.6%	39.7%	0.1%
C/PPS-4	5.0432	2.0473	4.1244	40.6%	40.0%	-0.6%
C/PPS-5	5.0892	2.0157	4.1421	39.6%	38.7%	-0.9%
Neat PPS	4.7985	--	3.3412	--	--	--

Table 6. The carbon fiber content results for one batch of carbon fiber PP samples by the ASTM burn off in air method.

Sample	Total mass (g)	Carbon Fiber mass (g)	Residue mass (g)	Nominal Fiber Content	Fiber Content from ASTM burn off in air	Deviation
C/PP-1	4.132	0.7752	0.8032	18.8%	19.4%	0.7%
C/PP-2	4.1672	0.7857	0.8156	18.9%	19.6%	0.7%
C/PP-3	4.0321	0.7512	0.7943	18.6%	19.7%	1.1%
C/PP-4	4.1987	0.7869	0.8212	18.7%	19.6%	0.8%
C/PP-5	4.2012	0.7612	0.7982	18.1%	19.0%	0.9%

Table 7. The carbon fiber content results for one batch of carbon fiber PP samples by the ASTM burn off in air method.

Sample	Total mass (g)	Carbon Fiber mass (g)	Residue mass (g)	Nominal Fiber Content	Fiber Content from ASTM burn off in air	Deviation
C/PPS-1	5.1324	2.0192	3.1594	39.3%	61.6%	22.2%
C/PPS-2	5.1245	1.9790	3.1321	38.6%	61.1%	22.5%
C/PPS-3	5.1732	2.0217	3.2532	39.1%	62.9%	23.8%
C/PPS-4	5.1543	2.0473	3.1723	39.7%	61.5%	21.8%
C/PPS-5	5.2173	2.0157	3.2004	38.6%	61.3%	22.7%

Table 8. Carbon fiber content results from the microscopic method.

Sample	Carbon Fiber Area Content	Carbon Fiber Mass content	Nominal Fiber Content	Deviation
C/PP	15.1%	21.1%	18.5%	2.6%
C/PPS	30.3%	34.5%	39.6%	5.1%

Figures
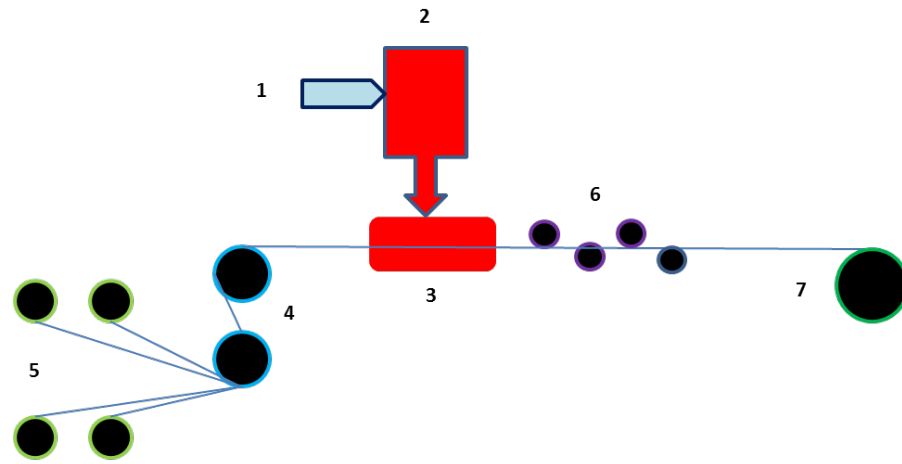
1：polymer supply;2: extruder;3: impregnator (heating die);
4: preheating rollers;5: fiber creels;6: hot compactors;7: puller

Figure 1. The hot melt impregnation process.
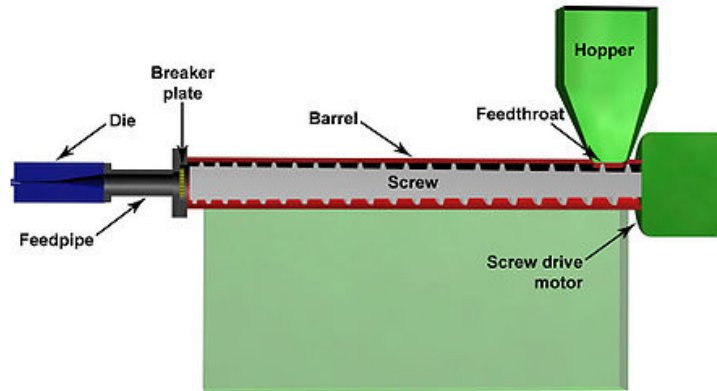
Figure 2. The extruder.
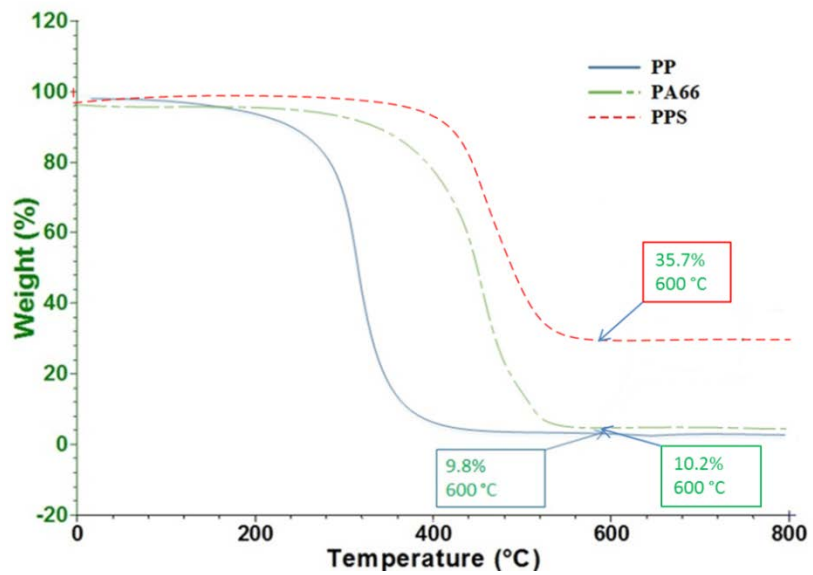
Figure 3. TGA plot of the mass loss of PP, PA66 and PPS resins heated up to 800°C.
Note that the resin still has residue at 600°C in nitrogen.

Figure 4. (a) Carbon fiber thermoplastic composite sample with known nominal fiber content before carbonization; (b) residue from composite sample after CIN; (c) residue from the *reference neat resin* after CIN.
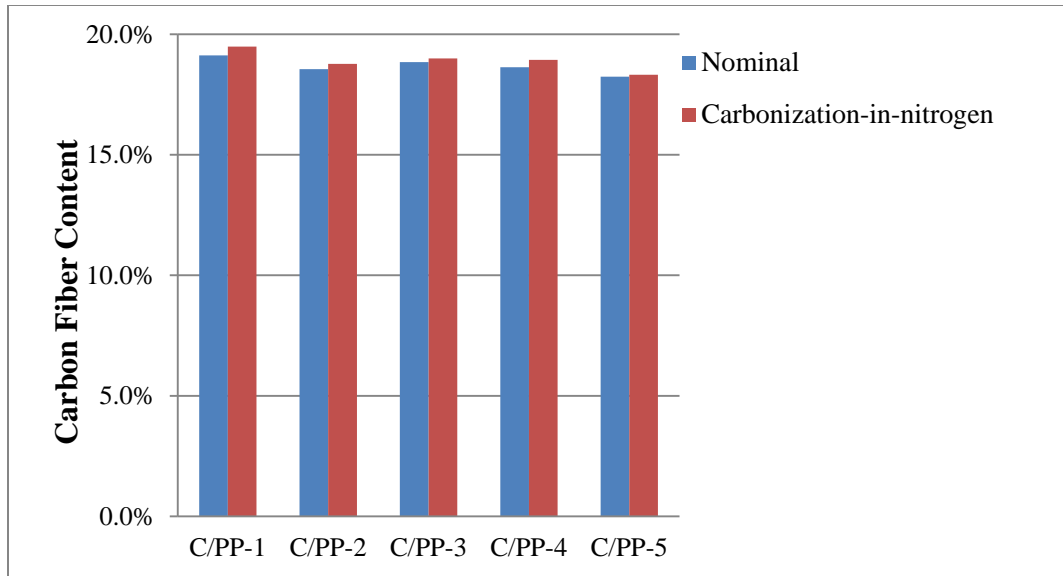
Figure 5. Comparison between fiber content from CIN and nominal fiber content in a batch of five carbon fiber PP samples.
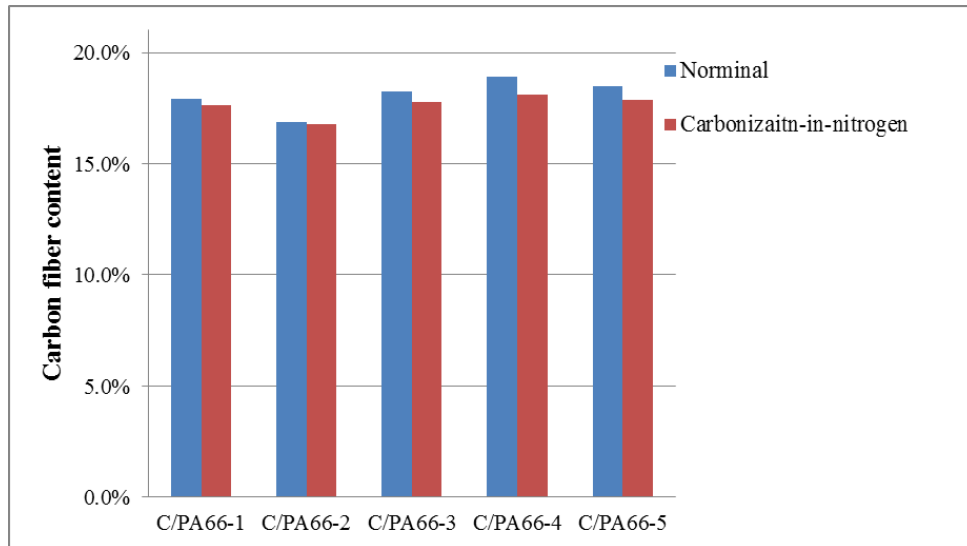
Figure 6. Comparison between fiber content from CIN and nominal fiber content in a batch of five carbon fiber PA66 samples.
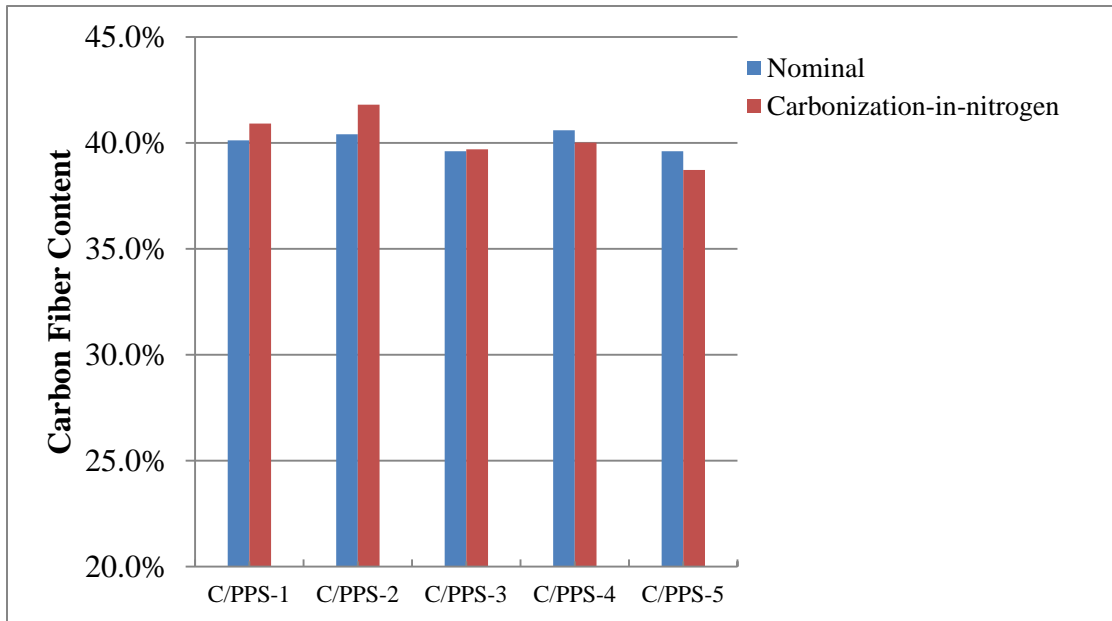
Figure 7. Comparison between fiber content from CIN and nominal fiber content in a batch of five carbon fiber PPS samples.
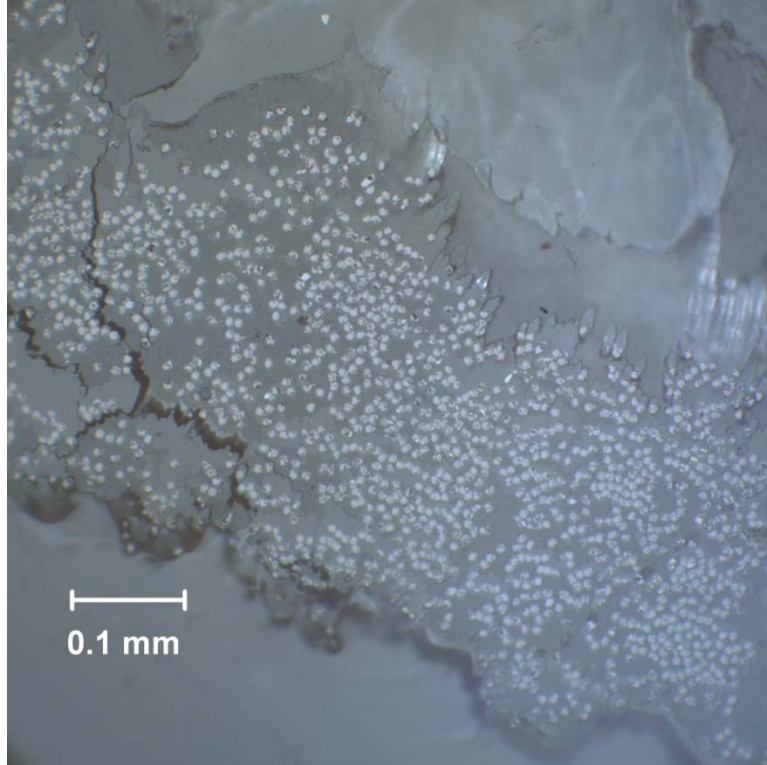
Figure 8. A typical microscopic image of a polished carbon fiber PP sample.
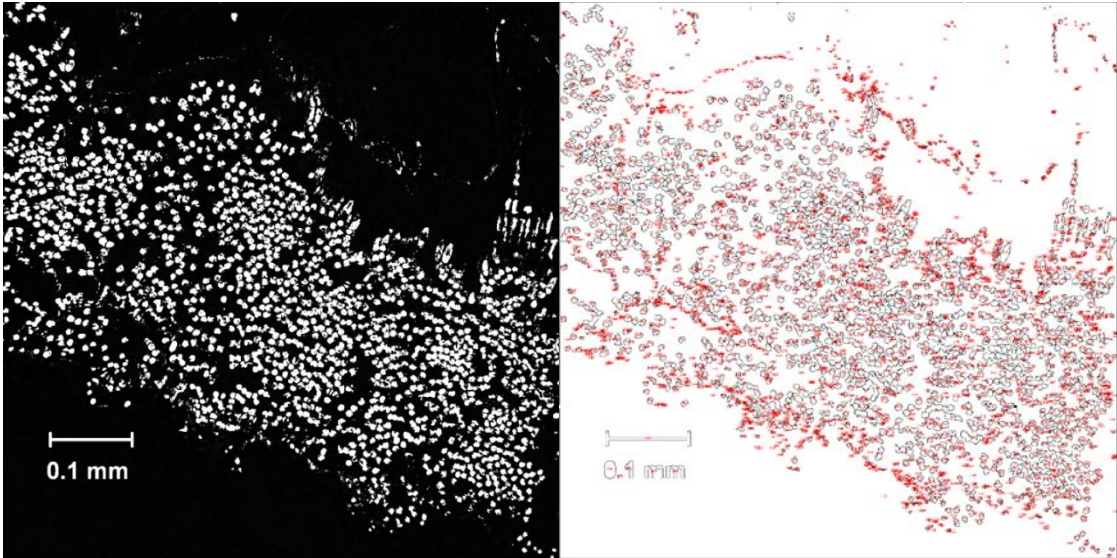
Figure 9. Carbon fiber PP sample.

DETERMINATION OF THERMAL DEGRADATION KINETIC PARAMETERS OF
CARBON FIBER REINFORCED PPS USING TGA

by

QIUSHI WANG
HAIBIN NING
UDAY VAIDYA
SELVUM PILLAY

DETERMINATION OF THERMAL DEGRADATION KINETIC PARAMETERS OF CARBON FIBER REINFORCED PPS USING TGA

Abstract

The mechanism and the kinetic model of the thermal degradation behavior of carbon fiber reinforced poly (phenylene sulfide) (CPPS) is studied by thermogravimetric analysis. The CPPS is subjected to thermogravimetric analysis (TGA) in air and nitrogen atmospheres at heating rates from 5 to 40°C min^{-1}. The TGA curves achieved in air are different from those obtained in nitrogen, demonstrating that weight loss occurs in a single stage in nitrogen while in two stages in air. To elucidate this difference, thermal decomposition kinetics are analyzed by applying the Kissinger, Flynn-Wall-Ozawa, Coat-Redfern and Malek methods. The activation energy () of the solid-state process is determined to be 202 kJ mol^{-1} in an oxidative atmosphere using Kissinger's method, which is 10-15 kJ mol^{-1} higher than the results calculated in nitrogen atmosphere.

The value of the activation energy obtained using the Ozawa-Flynn method is in agreement with that using Kissinger method. Different degradation mechanisms are used to compare with this value. Based on the analytical results from the Coat-Redfern and Malek methods, the actual thermal degradation mechanism of CPPS is a deceleration type. The carbonization behavior of CPPS exhibits the same temperature range as neat PPS.

Keywords: Thermal degradation; Carbon fiber; Poly (phenylene sulfide); Activation energies

Introduction

Carbon fiber reinforced polymers (CFRPs) have been manufactured during the last few decades to develop materials that combine high stiffness and strength with low density. This combination of properties has led to a strong increase in their use in the aeronautic, automotive, and energy sectors, replacing traditional materials such as steel, aluminum, and wood, amongst others.

The most widely-used high-performance thermoplastics are poly (etherether ketone) (PEEK), poly (phenylene supplied) (PPS), and poly (etherimide) (PEI). PPS is a semicrystalline polymer composed of phenyl rings and sulfur atoms that possesses outstanding mechanical and thermal properties. Composite structures made of PPS remain hard, impact-resistant, stiff, and dimensionally stable even when exposed to temperatures greater than 100°C. They are also resistant to aggressive media, possess inherent flame retardancy, absorb minimum water, and have excellent anti-aging and friction properties [1-3]. This is the reason why it has been evaluated recently as a replacement for conventional thermally-durable materials and components used in packaging and automobiles. In the aircraft industry, carbon fiber reinforced PPS (CPPS) is mainly used in structural applications, such as in J-Nose wing substructures of the Airbus A340-500/600[4].

Knowledge of the thermal degradation behavior of the CPPS becomes crucial since processing it at high temperatures may produce changes that would affect the ultimate performance. Therefore, the studies of its thermal degradation behavior and mechanism will be of paramount importance for process and performance evaluation.

Thermal degradation of PPS polymer has frequently been investigated. Montando et al. used carbonization-mass to observe the thermal carbonization of PPS with different structures [5]. Zongying et al. used FTIR to observe the isothermal cracking of PPS in air and nitrogen between 320 and 400°C [6]. Montando et al. used Py-MS to analyze the thermal degradation mechanism and pyrolysates of PPS with different substituted groups [7]. However, the relationships between the detailed mechanisms and kinetics of the carbon fiber reinforced PPS composites thermal degradation are not fully clear due to the complexity of the thermal degradation behavior. In this article, the thermal degradation of CPPS is investigated with thermagravimetric analysis (TGA). TGA is an excellent tool for studying the kinetics of thermal mechanisms. It provides information on the frequency factor, activation energy, and the overall reaction order.

There are two objectives in this study. One objective is to investigate the kinetics of the thermal degradation of CPPS using different kinetic methods. This thermal stability is described by comparing the temperature when degradation begins or by comparing the mass loss at a specific temperature when the tests are conducted in an air or nitrogen atmosphere. Moreover, apparent kinetic parameters are determined. The activation energy has been evaluated by employing Kissinger's method or Ozawa's method, which gives the estimated activation energy for the overall degradation. The second objective is to investigate the thermal degradation mechanism as a solid-state process. The kinetic parameters, obtained from different kinetic methods, are compared and discussed. The experimental results are compared to the pre-exponential factor and maser curves in the Coat-Redfern and Malek methods, respectively. The actual reaction mechanism is derived from those data.

Experiment

2.1Materials

The material investigated is Celstran PPS-CF40-1 (carbon fiber reinforced PPS) manufactured by Celanese Company. The carbon fiber weight fraction of the composite sample is 40 wt. % and the density is 1.49 g/cm^3. The glass transition temperature is between 90-100 °C by modulated DSC. Samples with a mass around 15 mg were desiccated in the oven at 60°C for 96 hours before the test.

2.2 Thermogravimetric Studies

Thermogravimetric analysis was performed using DuPont 2950 (TA Instrument) thermal analyzer. Conventional constant heating rate TGA measurements were run at 5, 10, 20 and 40 C min^{-1} in nitrogen or air atmosphere from ambient to 900 °C at a flow rate of 50 ml min^{-1}.

The general form of the kinetic expression used in analyzing dynamic and isothermal TGA data is based on n^{th} order reaction mechanism. In most cases, all kinetic studies assume that the isothermal rate of conversion[8], da/dt, is a linear function of the reactant concentration loss and of the temperature-independent function of the conversion, α, that is

$$\frac{da}{dt} = kf(\alpha) \tag{1}$$

where α is the reaction rate which is defined as the derivative of the conversion with respect to time. $f(\alpha)$ depends on the mechanism of the degradation reaction. The function k is always described by the Arrhenius expression:

$$k = Ae^{-\frac{E}{RT}} \tag{2}$$

Where A, the pre-exponential factor (min^{-1}), is assumed to be independent of temperature, E_a is the activation energy (kJ mol⁻¹), T is the absolute temperature (K) and R is the gas constant ($8.314J \cdot mol^{-1} \cdot k^{-1}$).

If the sample temperature is changed by a controlled and constant heating rate, $\beta = dT/dt$, the variation in the degree of conversion can be analyzed as a function of temperature, which depends on the time of heating. Therefore, the reaction rate may be written as follows:

$$\frac{d\alpha}{dT} = \frac{A}{E}e^{-\frac{E}{RT}}f(\alpha) \tag{3}$$

Integration of this equation from an initial temperature, T_0, corresponding to a degree of conversion α_0, to the peak temperature, T_P, where $\alpha = \alpha_P$, gives:

$$\int_{\alpha_0}^{\alpha_P} \frac{d\alpha}{f(\alpha)} = \frac{A}{\beta}\int_{T_0}^{T_P} e^{-\frac{E}{RT}} dT \tag{4}$$

When T_0 is low enough, $\alpha_0 = 0$, so there is no reaction between 0 and T_0;

$$g(\alpha) = \int_0^{\alpha_P} \frac{d\alpha}{f(\alpha)} = \frac{A}{\beta}\int_0^{T_P} e^{-\frac{E}{RT}} dT \tag{5}$$

where $g(\alpha)$ is the integral function of conversion, which is either a sigmoidal function or a deceleration function. Table 1 shows different expression for $g(\alpha)$ and $f(\alpha)$ for the different solid state mechanisms [8]. The functions were satisfactorily used for the estimation of the reaction solid-state mechanism from non-isothermal TG experiments.

Kissinger method – Differential method

The Kissinger method has been used in this work to determine the activation energy of solid state reactions from plots of the logarithm of the heating rate versus the inverse of the temperature at the maximum reaction rate in constant heating rate experiments [9].

The Kissinger method is based on the calculation of the apparent activation energy E on the temperature at which the maximum rate of weight loss, T_{max} occurs in the TGA cure at several rates.

The Kissinger equation is

$$\ln\frac{\beta}{T_m^2} = \ln[An(1-X)_m^{-1}] - \left\{\frac{E}{RT_m}\right\} \tag{6}$$

Where β is the heating rate, A is the pre-exponential factor, n is the order of the reaction and R is the universal gas constant. A plot of $\ln\beta/T_m^2$ versus ($1/T_m$) then gives $-E/R$ from the slope of the line.

Flynn-Wall-Ozawa Method-Integral method

This method is based on the representation of the degradation reaction by power law kinetics [10]. This method used the approximation of Doyle to evaluate the integrated form of the rate equation and yields eq. (3) as an approximate solution [11]. The authors supposed that $\ln(1 - 2RT/E)$ tend to be zero for the Doyle approximation obtaining in natural logarithmic form. Assuming E/RT >20, it can be obtained:

$$\log(\beta) = \log\frac{AE}{g(\alpha)R} - 2.135 - \frac{0.4567E}{RT} \tag{7}$$

where $g(\alpha)$ represents the weight loss function. E is obtain from a plot of $\log(\beta)$ versus 1000/T for fixed degrees of conversion and the slope of the line is given by $0.4567E/R$.

Coat-Redfern method

Coats-Redfern method uses an asymptotic approximation for resolution of Equation.5 [12]. Based on the Doyle approximation that $\ln(1-2RT/E)$ tends to be zero, the logarithmic form could be attained as following:

$$\ln\frac{g(\alpha)}{T^2} = \ln\frac{AR}{\beta E} - \frac{E}{RT} \qquad (8)$$

The parameters for the different degradation process $g(\alpha)$ could be achieved from the Table 1. The activation energy could be generated from the plot of $\ln(g(\alpha)/T^2)$ versus $1000/T$.

Malek method for determination of reaction mechanism

The activation energy of a solid state reaction can be determined from several non-isothermal measurements, whatever the reaction mechanism. If the value of the activation energy is known, the kinetic model of the process can be found in the following way [13, 14]. Malek method defines the function:

$$z(\alpha) = \frac{\left(\frac{d\alpha}{dt}\right)}{\beta}\pi(x)T \qquad (9)$$

Where $z(\alpha) = E/RT$, and $\pi(x)$ is an approximation of the temperature integral which cannot be expressed in a simple analytical form. In this study we used the fourth rational expression of the Senum and Yong [18, 19], which gives errors lower than 10^{-5} for x =20. From Equations (1) and (9) we obtain

$$z(\alpha) = f(\alpha)g(\alpha) \tag{10}$$

The master plots corresponding to Equation. (10) are shown in Figure 5.

Comparing the experimental curve calculated from Equation (10) with the master curve will reflect the mechanism of thermal degradation of the reaction.

Results

TGA experiments in air or nitrogen flow at heating rates of 5, 10, 20, and 40 °C min^{-1} are shown in Figure 1 and Figure 2. Mass is lost as temperature increases, and a lower heating rate yields earlier degradation onsets. Mass loss is around 60% in an oxidative atmosphere while the char yield obtained in nitrogen at 900°C is dependent on heating rate. These TGA curves correspond to a single-stage decomposition reaction in nitrogen but a two-stage reaction while in air. The procedural decomposition temperature (initial and final) (T_i and T_f) are well defined. The temperature of the maximum rate (T_{max}) and char yield (wt. %) at 900 are shown in these curves. The values of T_i , T_f and T_{max} are listed in Table 2.

In an inert atmosphere the degradation stage begins at 415.5°C and ends at 593.8°C. The maximum rate is near 530°C and the corresponding mean mass loss of the stage at this temperature was about 4.5 %, as shown in Table 2. However, the mass loss is dependent on the heating rate in the nitrogen atmosphere. Table 3 shows a mass loss between 3.5 and 5.5 mass% for experiments run from 5 to 40 °C min^{-1}.

Two stages were observed for the samples in oxidative conditions. The first stage begins at about 445.5°C and weight loss is 6 mass% of the sample's initial mass. The second stage shows a maximum rate at 545.5°C. This stage corresponds to the degradation of the

residue with a rapid rate. The global mass loss of the second stage is close to 35% of the initial mass.

Figure 3 shows the TGA results of PPS and CPPS in the nitrogen atmosphere at the heating rate of 20°C min^{-1}. In this Figure, neat PPS displays a single degradation stage that initiates at 405°C and shows the T_{max} around 530°C. The residual mass was about 36% of the initial weight. However, in the case of CPPS, the composites display similar degradation curves to the neat polymers (with the same major mass fragments), albeit shifted to higher temperatures. T_i and T_{max} increased by about 35°C and 60°C, respectively. Moreover, the residual weight also increased in comparison to the neat polymers.

Employing Kissinger's method and the experimental data recorded in Figure 1 and 2, the activation energy of the decomposition of CPPS was calculated from a straight line fit of a plot of $\ln(\beta/T_m^2)$ versus $(1000/T_m)$ (Figure 4). The value obtained from the Kissinger's plot was summarized in Table 4 for both atmospheres. The activation energy value calculated in the nitrogen is around 189 $kJ\ mol^{-1}$, which is lower than the E_a obtained in the air environment. The difference is about 10 $kJ\ mol^{-1}$ for the equivalent mass loss during the first stage. These results suggest a different comprehensive degradation mechanism in which an oxidative stage was involved. The E_a was estimated to be around 165 $kJ\ mol^{-1}$ for the second stages.

The Flynn-Wall-Ozawa method was involved in employing the overall apparent activation energy by using the linear fitting of $\log(\beta)$ versus 1000/T from Equation 7. This method is based on the assumption that the reaction model is independent of the

heating rate. From the Doyle approximation, only conversion values in the range 5-20% can be used. Therefore, 5, 9, 12, 17, and 20% were used. The results of the Flynn-Wall-Ozawa method are presented in Figure 5. The nearly parallel fitting lines indicate a constant activation energy range of conversion analysis and confirm the validity of the approach used. Table 5 shows the E_a values corresponding to the different conversions. The mean value is around 205 $kJ\ mol^{-1}$ in the air and 190 $kJ\ mol^{-1}$ in the nitrogen. The values have a good agreement with the value from the Kissinger's method in Table 4.

The Kissinger and Flynn-Wall-Ozawa methods present the advantage of determining the activation energy from TGA results directly. However, these values will not directly indicate the thermal degradation kinetic model of the CPPS. The kinetic model can be obtained by combining the previous results with Coat-Redfern and Malek master curves.

In the Coats-Redfern method, the activation energy corresponding to different g(α) for sigmoidal and decelerated mechanisms (Table 1) can be achieved at constant heating rate using the linear fitting plot of $\ln{(g(\alpha)/T^2)}$ versus $1000/T$. By integrating the previous results from Table 4 and 5, the activation energies and the correlations for the conversion at constant heating rate values can be achieved, as shown in Table 6, by the Coats-Redfern Method. Analysis of these data indicates that the activation energies which are in best agreement with those obtained by Kissinger's method correspond to a D_n type mechanism both in air and nitrogen atmosphere. For comparison, the Flynn-Wall-Ozawa method was chosen because it is independent of a particular mechanism. It was found that the activation energies from the heating rate 10 °C min^{-1}, 209 $kJ\ mol^{-1}$, had a great agreement with the values in Table 6 which were obtained from the Coats-Redfern method. Since the value corresponds to 209 $kJ\ mol^{-1}$ in the Coats-Redfern, it is

suggested that the solid-state thermal degradation mechanism is a deceleration (D_n)type. This indicates that the CPPS has the same type of degradation mechanism.

The Malek method was chosen to confirm the deceleration behavior by comparing the reference theoretical master curves with the experimental data. Figure 6 demonstrates the master curve plots $z(\alpha)$ versus α . Only conversion values in the range 5-20% were considered for discussion because of the Doyle approximation. In Figure 6, the experimental results show a better match with the $z(D_2)$ master curve, which corresponds to a deceleration D_2 and D_3 mechanism.

Discussion

The thermal degradation of PPS polymers is usually illustrated as one-stage [16]. The major pyrolystates of PPS were benzenethiol and H$_2$S. The major mechanisms included depolymerization, main chain random scission, and carbonization. The initial scission of PPS was depolymerization and main chain random scission to evolve benzenethiol and hydrogen sulfide, respectively, as major products; while depolymerization dominated in lower temperature carbonization and main chain random scission dominated in higher temperature. The chain transfer of carbonization also produced in initial carbonization and gradually dominated at higher carbonization temperatures to form the high char yield of solid residue.

In an oxidation atmosphere, the CPPS exhibits two clear steps, which led to the total decomposition of the material; the first related to the scission of the polymeric chains and the second to the decomposition of aromatic structures that remained in the residue under inert atmosphere. T_i and T_{max} of the first step are around 455°C and 535°C, slightly

higher than in the nitrogen environment, which is ascribed to the oxygen-stabilizing function[16]. The function can be described as follows: the depolymerization happens along with the radials formed with oxygen to develop a new polymer radical. The peroxide radical is more thermally stable than the polymer degraded in the absence of oxygen. This explains why the activation energy in the air is $10 \: kJ \: mol^{-1}$ higher than in the nitrogen atmosphere for the first stage, and why the initial degradation temperature in the air is around 30°C higher than in the nitrogen. When all the peroxide radical cores have been eliminated, the degradation of PPS jumped to the final carbonization stage.

When compare the PPS and CPPS TGA results, the CPPS shows better thermal stability. The CPPS displays similar degradation curves to the PPS, albeit shifted to higher temperatures. In both curves, the residue weight appeared to remain constant above 535 °C and the char yield was at a constant value, indicating that carbonization played an important role in the final thermal degradation process. The thermal stability enhancement attained is ascribed to both the high thermal conductivity of the carbon fiber (compared to PPS resin), which allows rapid heat transport and enables excessive radial heat radiation. Moreover, the carbon fiber caused a barrier effect, hindering the diffusion of the degradation products from the bulk of the polymer to the gas phase, hence slowing down the decomposition process. Analogous stability effects have been reports in the literature for polyimide/carbon fiber composites [16].

Brown and Kashiwagi [17] explained the stabilizing effect of oxygen in the degradation process. The oxygen attacks hydrogen-activated groups to form a hydroperoxide which undergoes a scission and gives a hydroxyl-terminated polymer and products which contain carbonyl functions. Oxygen also promotes random scission. The process is

accompanied by the elimination of different chemical species (water, ester). The activation energy decreases to $165\ kJ\ mol^{-1}$, corresponding to the decomposition of unvolatile residue, which results from the first stages and the oxygen promoting benefit.

Conclusion

The kinetic parameters and the degradation mechanism of PPS and C/PPS using TGA experiments have been studied to explain CPPS thermal degradation in air or nitrogen, based on the activation energy calculation. The thermal degradation mechanism for CPPS is a deceleration (D_n) type, which is a solid-stage process based on an n-dimensional diffusion both in air and nitrogen atmospheres. The degradation behavior of CPPS in the nitrogen atmosphere is a single-stage process and the activation energy is around 189 $kJ\ mol^{-1}$, whilst in the air it is a two-stage thermal degradation process. The activation energy for the first step is 202 $kJ\ mol^{-1}$ and 165 $kJ\ mol^{-1}$ for the second step in the air atmosphere. The PPS and the CPPS possess the same carbonization behavior and have the same carbonization temperature range (above 535°C) from the thermal degradation study of CPPS and PPS.

Acknowledgements

References

[1] Jiri G. D. Handbook of Thermoplastic Elastomers, Second Edition, 2014, P301-337

[2] George Marsh Reinforced Plastic, 2014; (58):161-169.

[3] Ning H, Vaidya U, Janowski GM, Husman G. Compos Structure 2007; 80(1) 105-16.

[4] Diaz J, Rubio L. J Mater Process Technol 2003; (342-6):143-144.

[5] Montaudo G, Przybylshi M, Ringsdorf. Makromol Chemie 1975; (176):1761.

[6] Du Zongying J. Sichuan Univ Natural Sci 1987; 24:111.

[7] Montaudo G, Puglisi C, Samperi F. J Polym Sci, Part A: Polym Chem 1997; (118):1149.

[8] Vyazovkin S. Int Reviews in Physical Chemical 2000; 19(1):45.

[9] Kissinger HE. Anal Chem 1957; (29):1702-6.

[10] Ozawa T. Bull Chem Soc Jpn 1965; 38(11): 1881-6.

[11] Doyle CD. J Apl Rolym Sci 1961; 5(15): 285-92.

[12] Coats AW, Redfern JP. Nature 1964; 201(4914): 68-9.

[13] Malek J. Thermochim Acta 1989; 138(1-2): 337-46

[14] Criado JM, Malek J, Ortage A. Thermochim Acta 1989; 147(1-2): 377-85.

[15] Abate L., Bottino F. A., Calanna S. and Pollicino A.. Polymer, 1999; (40): 2719.

[16] Perng L. H.. Polymer Degradation and Stability, 2000; (69): 323-332.

[17] Peterson J.D., Vyazovkin S. and Wight C.. J. Phys. Chem. B, 1999; (103): 8087.
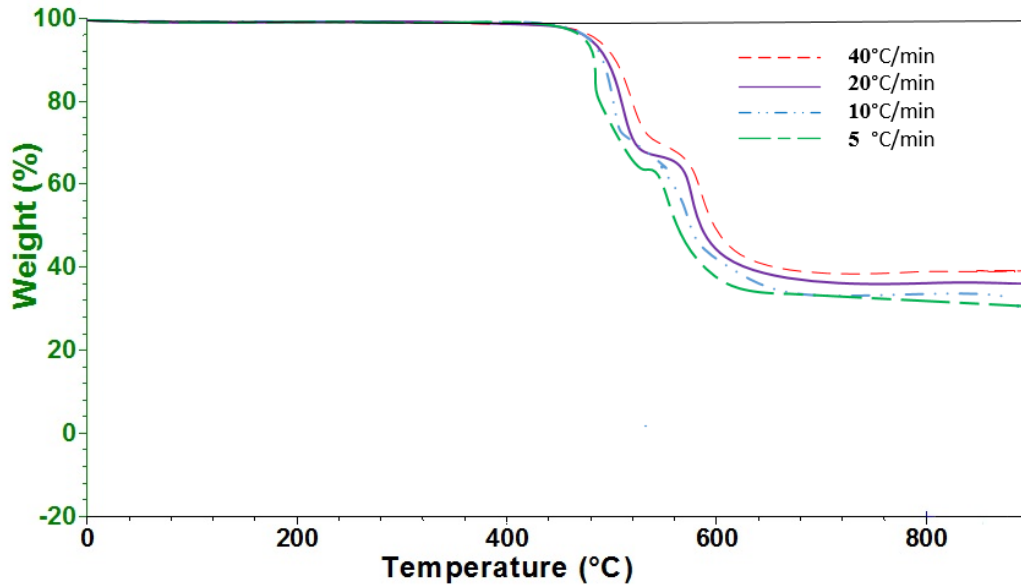
Figure 2. TGA of CPPS composite in the air atmosphere at different heating rates.
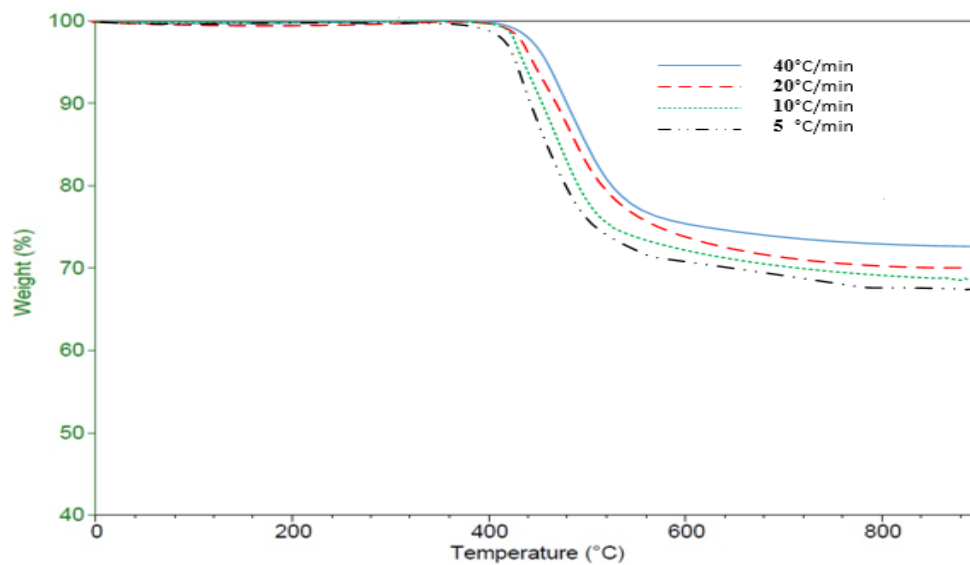
Figure 2. TGA of CPPS composite in the nitrogen atmosphere at different heating rates.

Figure 3. Comparison of TGA between CPPS and PPS in the nitrogen at heating rate 20°C min^{-1}.

Figure 4. Kissinger plots of CPPS composite in nitrogen

Figure 5.Typical plots of $\log(\beta)$ versus 1000/T at various conversion values in the range 5-20%.

Figure 6.The comparison between master curve (black) and experiment data calculated by Eqn. (10) (Red)

Tables

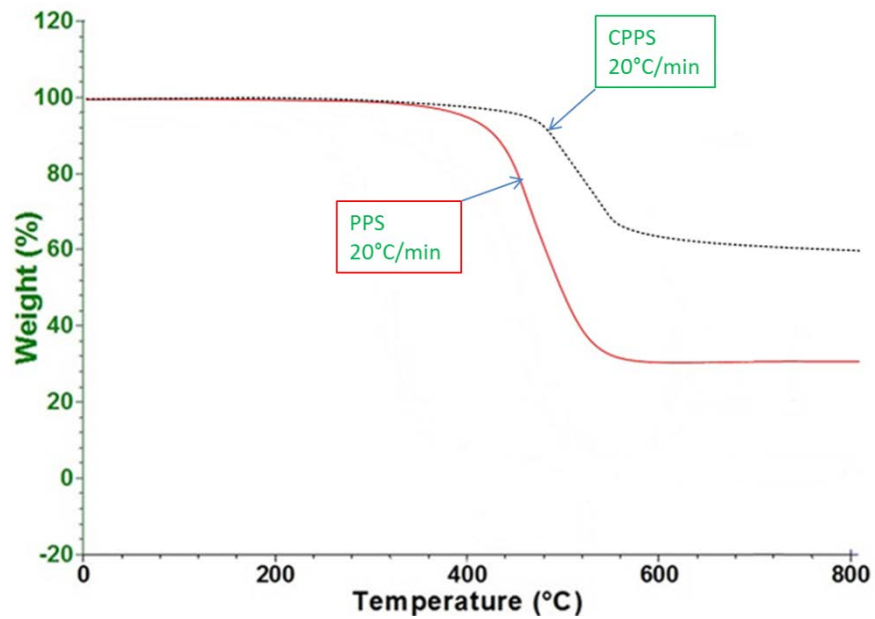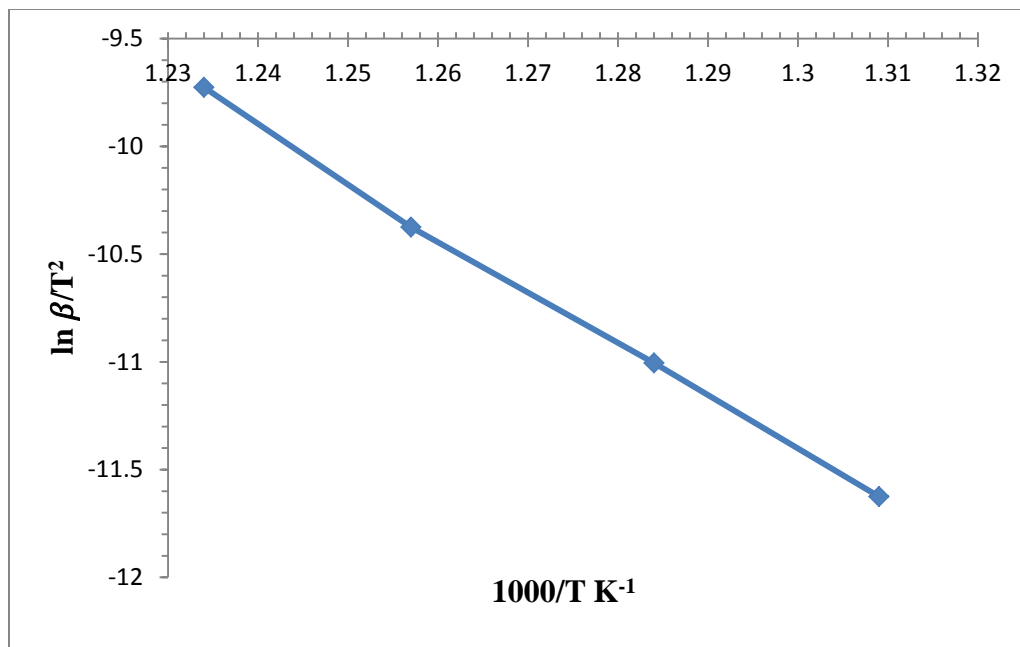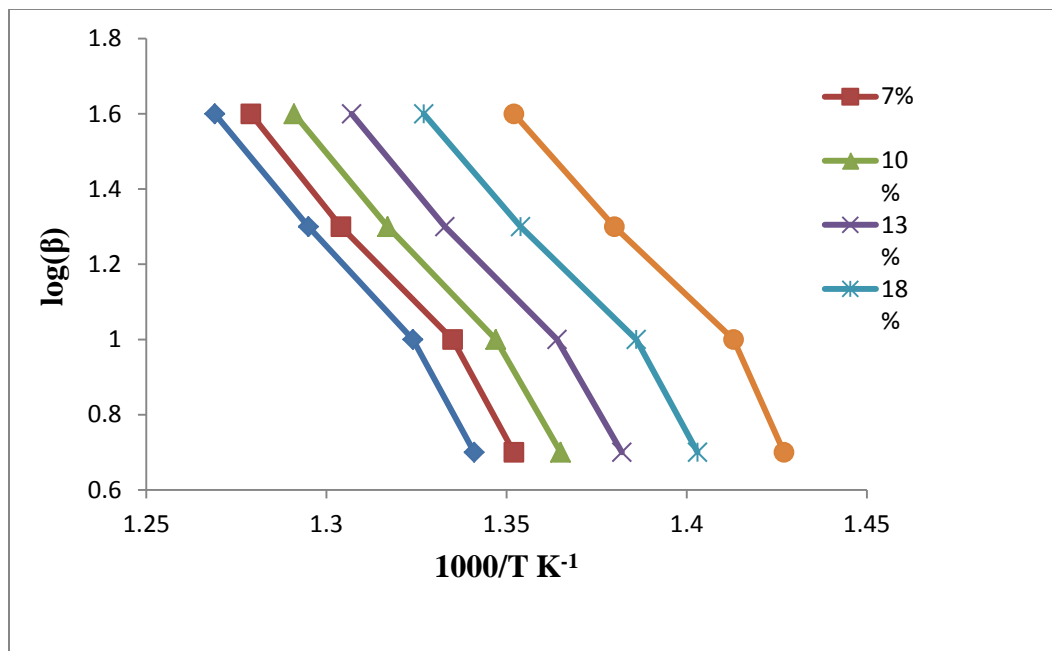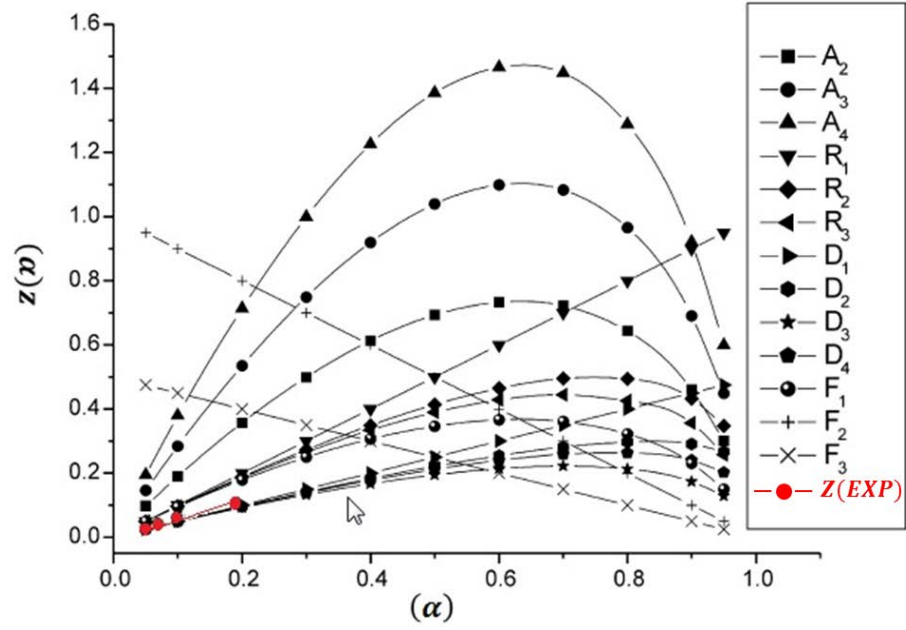Table 1 .Algebraic expressions for the most frequently used mechanisms of solid-state processes.

Symbol	$f(\alpha)$	$g(\alpha)$	Solid-state processes
Sigmoidal curves			
A_2	$2(1-\alpha)[\ln(1-\alpha)]^{-1}$	$[-\ln(1-\alpha)]^{1/2}$	Nucleation and growth
A_3	$3(1-\alpha)[\ln(1-\alpha)]^{-1/2}$	$[-\ln(1-\alpha)]^{1/3}$	Nucleation and growth
A_4	$4(1-\alpha)[\ln(1-\alpha)]^{-1/3}$	$[-\ln(1-\alpha)]^{1/4}$	Nucleation and growth
Deceleration curves			
R_1	1	α	Phased boundary controlled reaction
R_2	$2(1-\alpha)^{1/2}$	$[1-\ln(1-\alpha)]^{1/2}$	Phased boundary controlled reaction
R_3	$3(1-\alpha)^{2/3}$	$[1-\ln(1-\alpha)]^{1/3}$	Phased boundary controlled reaction
D_1	$1/(2\alpha)$	α^2	One-dimensional diffusion
D_2	$-1/\ln(1-\alpha)$	$(1-\alpha)\ln(1-\alpha)+\alpha$	Two-dimensional diffusion
D_3	$3(1-\alpha)^{2/3}/2[1-(1-\alpha)^{1/3}]$	$[1-(1-\alpha)^{1/3}]^2$	Three-dimensional diffusion
D_4	$3/2[(1-\alpha)^{-1/3}-1]$	$(1-2/3\alpha)-(1-\alpha)^{2/3}$	Three –dimensional diffusion
F_1	$(1-\alpha)$	$\ln(1-\alpha)$	Random nucleation with one nuclei
F_2	$(1-\alpha)^2$	$1/(1-\alpha)$	Random nucleation with two nuclei
F_3	$1/2(1-\alpha)^3$	$1/(1-\alpha)^2$	Random nucleation with three nuclei

Table 2. The temperature (initial, final and max) and Char yield at 900°C at different heating rates.

Atmosphere	Heating rate (°C min^{-1})	T_i(°C)		T_{max}(°C)		T_f(°C)		Char yield 900°C (wt. %)
Nitrogen	5	415.5		515.8		562.5		72.1
	10	426.6		528.7		568.8		72.5
	20	435.2		537.6		570.6		74.5
	40	445.5		548.5		593.8		77.8
Air		T_{1i}(°C)	T_{2i}(°C)	T_{1max}(°C)	T_{2max}(°C)	T_{1f}(°C)	T_{2f}(°C)	
	5	445.5	532.5	506.5	542.5	532.5	551.5	36.8
	10	459.5	535.2	507.5	543.5	535.2	558.6	37.5
	20	467.5	547.5	517.7	554.5	547.5	567.8	39.8
	40	468.5	557.4	523.5	567.5	557.4	575.6	41.5

Table 3. Mass loss (%) of CPPS composite for each step of dynamic TGA in air or inert atmosphere.

Heating rate (°C min^{-1})	Nitrogen (wt. %)	Air (wt. %)	
		Step 1	Step 2
5	5.5	6.5	35.3
10	4.2	5.8	32.4
20	3.8	5.2	31.7
40	3.5	4.8	30.9

Table 4. Kinetic parameters calculated from Kissinger equation for the degradation of CPPS composite in nitrogen and air flow.

Atmosphere	$\beta(^\circ C\ min^{-1})$	E/R	$\ln A$	R^2	$E_a(kJ\ mol^{-1})$
Nitrogen	5-40	22.37	15.9	0.9962	189
Air	5-40	24.4	12.7	0.9974	202
		19.8	3.2	0.9965	165

Table 5. The activation energies obtained by the Ozawa Method in air and nitrogen

$\alpha(\%)$	Air		Nitrogen	
	$E_a(kJ\ mol^{-1})$	R^2	$E_a(kJ\ mol^{-1})$	R^2
5	227	0.9956	218	0.9967
9	225	0.9978	209	0.9987
12	208	0.9969	195	0.9973
17	195	0.9932	187	0.9953
20	185	0.9934	175	0.9934
30	178	0.9987	--	--
40	176	0.9981	--	--
50	165	0.9915	--	--
55	154	0.9965	--	--

Table 6. Activation energies obtained using the Coats-Redfern method for the thermal degradation of the CPPS at different heating rate in nitrogen.

Mechanism	5 (°C min⁻¹)		10 (°C min⁻¹)		20 (°C min⁻¹)		40 (°C min⁻¹)	
	$E_a(kJ\ mol^{-1})$	R^2	$E_a(kJ\ mol^{-1})$	R^2	$E_a(kJ\ mol^{-1})$	R^2	$E_a(kJ\ mol^{-1})$	R^2
A_2	53	0.9967	75	0.9953	76	0.9953	80	0.9953
A_3	32	0.9987	45	0.9934	47	0.9934	51	0.9934
A_4	25	0.9973	37	0.9956	35	0.9956	46	0.9956
R_1	117	0.9953	135	0.9978	156	0.9978	145	0.9978
R_2	119	0.9934	137	0.9987	148	0.9987	158	0.9987
R_3	168	0.9956	176	0.9973	176	0.9973	178	0.9973
D_1	182	0.9978	189	0.9987	199	0.9987	208	0.9987
D_2	189	0.9969	209	0.9973	209	0.9973	211	0.9973
D_3	117	0.9932	140	0.9953	187	0.9953	196	0.9953
D_4	109	0.9934	143	0.9934	165	0.9987	134	0.9987
F_1	27	0.9987	40	0.9956	45	0.9973	55	0.9973
F_2	33	0.9981	43	0.9934	50	0.9953	60	0.9953
F_3	57	0.9915	78	0.9987	78	0.9953	87	0.9953

4. OVERALL SUMMARY AND CONCLUSIONS

A new carbonization-in-nitrogen method has been developed to measure the fiber content in carbon fiber thermoset matrix composites. A *reference neat resin* sample was carbonized with a carbon fiber thermoset composite sample under a nitrogen environment at a temperature ranging from 400°C to 600°C. The carbon fibers were protected from oxidization while the resin was carbonized. The carbonization rate of the reference neat resin sample was used to calculate the amount of the resin matrix in the composite sample. By comparing the nominal carbon fiber content with the NIC results, the deviations were found to be. The results from the carbonization-in-nitrogen method demonstrate that the method can be used as a generalized way to determine fiber content in carbon fiber reinforced thermoset composites effectively and accurately.

The accuracy and reliability of the carbonization-in-nitrogen method for measuring the carbon fiber content in the thermoplastics resin systems were assessed in this study. The merits of the carbonization-in-nitrogen method could be further amplified when applying it to the high-temperature-resistant and semi-crystallization thermoplastic PPS resin system. The low deviation between nominal and experimental results of different fiber-content ranges for different thermoplastic systems indicates the carbonization-in-nitrogen method could be extended to thermoplastic resin composites.

The degradation mechanism and kinetic parameters of the CPPS has been studied using TGA method both in air and nitrogen. The activation energy of the CPPS has been calculated and compared by different methods. It has been found that the thermal degradation kinetics of CPPS is a solid-stage process based on an n-dimensional diffusion both in air and nitrogen atmospheres. The degradation behavior of CPPS in the nitrogen

atmosphere is a single-stage process and the activation energy is around 189 kJ mol^{-1}. In the air, it is a two-stage thermal degradation process, with the activation energy for the first step being 202 kJ mol^{-1} and 165 kJ mol^{-1} for the second step for the oxygen stabilizing and promotes random scission benefits. The fundamental assumption of the carbonization-in-nitrogen method, that the carbonization of the reference neat resin and the resin in the composites possess the same carbonization behavior and have the same carbonization temperature range (above 535°C), has been validated from the thermal degradation study of CPPS and PPS.

5. FUTURE WORK

1. Apply the new method to other thermoset and thermoplastic systems to further confirm the accuracy of this method. Employ this method in other facilities by different operators to validate its universal property.

2. Study the thermal degradation behavior of the carbon fiber reinforced high-temperature-resistant thermoplastic composites such as PEEK and PEI to extract the appropriate carbonization temperature for this method. Create a carbonization temperature database of the commonly used thermoset and thermoplastic resin systems to further expand the convenience of the CIN method.

3. Extend this CIN method to carbon and glass fiber hybrid composites. A two-step processes may be needed. The first step is expected to be similar to the CIN process. The second step will involve burning off all of the carbon fibers and the resin matrix residue from the Step 1 sample. The burn off is expected to be done in the air at high temperature with the glass fiber only remaining.

GENERAL LIST OF REFERENCES

[1] Chawla KK. Composite materials science and engineering. New York: Springer-verglag, 1998

[2] Hufenbach W., Dobrzaski L.A., Gude M., Konieczny J., and Czulak A., Optimization of the rivet joints of the CFRP composite material and aluminum alloy, Journal of Achievements in Materials and Manufacturing Engineering, 2007; (20): 119-122.

[3] Jamroziak K., and Bocian M., Identification of composite materials at high speed deformation with the use of degenerated model, Journal of Achievements in Materials and Manufacturing Engineering, 2008; (28/2): 171-174.

[4] Komotori J., Shimizu M., and Miyano Y., Effects of the fiber content on the longitudinal tensile fracture behavior of uni-directional carbon/epoxy composites, Journal of Materials Processing Technology, 1997; (67): 89-93.

[5] Manson JAE ,. Composite processing and manufacturing- an overview. In: Comprehensive composite materials. Oxford, UK: Elsevier Science Ltd.; 200.p.577-607.

[6] Jiri George D, , Applications of Thermal Elastomers. Handbook of Thermoplastic Elastomers, Second Edition, 2014, P301-337

[7] Manson JAE , Walkman MD, Bernet N. Composite processing and manufacturing-an overview. In: Comprehensive composite materials. Oxford, UK: Elsevier Science Ltd.; 200.p.577-607.

[8] Ning H, Vaidya U, Janowski GM, Husman G. Design, manufacture and analysis of a thermoplastic composites frame structure for mass transit. Compos Structure 2007; 80(1) 105-16.

[9] Rubio L. Developments to manufacture structural aeronautical parts in carbon fiber reinforced thermoplastic materials. J Mater Process Technol 2003; 143-144:342-6.

[10] Jiri George Drobny, Applications of Thermal Elastomers. Handbook of Thermoplastic Elastomers, Second Edition, 2014, P301-337.

[11] Chen J.H., Schulz E., Bohse J., Hinrichsen G., Effect of fiber content on the interlaminar fracture toughness of unidirectional glass-fiber/polyamide composite, Composites A, 1999; (30): 747-755.

[12] Vaidya U. Composites for Automotive, Truck and Mass Transit: Materials , Design, Manufacturing. 2011

[13] Okoli, and G.F. Smith, Failure modes of fiber reinforced composites: The effect of strain rate and fiber content, Journal of Materials Science, 1998; (33): 5415-5422.

[14] Chen J.H., Schulz E., Bohse J., Hinrichsen G., Effect of fiber content on the interlaminar fracture toughness of unidirectional glass-fiber/polyamide composite, Composites A, 1999; (30): 747-755.

[15] Simon S. and Strunk L., Fibre volume of resin matrix composites by density measurement, Int. SAMPE Symp. Exihib. 1987; (32): 116-22.

[16] Daniel L. P. and Sovinski M.F., Determination of fiber volume in carbon/cyannate ester composites using thermogravimetric analysis (TGA), NASA/TM–2006–214143.

[17] Purslow D., On the optical assessment of the void content in composite materials, Composites, 1984; (15): 207–210.

[18] ASTM D3171 Test method for constituent content of composite materials. ASTM International, West Conchohocken, 2012.

[19] Cullis C.F. and Hirschler M.M. The combustion of Organic Polymers, Oxford University Press 2008;122(3): 122-243.

[20] Lyon R.E.. Polymer Degradation and Fire Hazard Review. Polymer degradation and stability. 1990; 30(1):3-12.

[21] HE J, Duan X. Study on the kinetics and mechanism of thermal degradation of PEEK by temperature programmed decomposition. Acto Chim Sin. 1997;55(12): 1152-7.

[22] Purslow D., On the optical assessment of the void content in composite materials, Composites, 15 (1984) 207–210.

[23] Daniel L. P. and Sovinski M.F., Determination of fiber volume in carbon/cyannate ester composites using thermogravimetric analysis (TGA), NASA/TM–2006–214143.

[24] Vyazovkin S. Kinetic concepts of thermally stimulated reactions in solids: A view from a historical perspective. Int Reviews in Physical Chemical 2000; 19(1):45.

[25] Kissinger HE. Reaction Rate of Processes Involving Solids with Different Specific Surfaces, Anal Chem 1957; 29:1702-6.

[26] Ozawa T. Reaction Kinetics in Differential Thermal Analysis, Bull Chem Soc Jpn 1965; 38(11): 1881-6.

[27] Doyle CD, Analytical Solution for the Kissinger Equation, J Apl Rolym Sci 1961; 5(15): 285-92.

[28] Coats AW, Redfern JP. Data Treatment in Non-isothermal Kinetics and Diagnostic Limits of Phenomenological Models, Nature 1964; 201(4914): 68-9.

[29] Malek J. Determine of Activation Energies of Chemical Reaction by Differential Thermal Aanlysis, Thermochim Acta 1989; 138(1-2): 337-46

[30] Criado JM, Malek J, Ortage A. Diagnostic Limits of Phenomenological Models of Heterogeneous Reactions and Thermal Analysis Kinetics, Thermochim Acta 1989; 147(1-2): 377-85.

[31] Mallick PK. Fiber-reinforced composite: materials, manufacturing, and design Boca Raton, FL CRC, 1998; 123 (2-4): 26-29.

[32] Gum, Riese,Ulrich, Research Polymers: Chermmistry, Technology, Applications and Markets. 1992; 233(3-5): 11-117

[33] May, C.A. and Newey H.A., Epoxy-Acrylic Resins for FRP structures. Proceedings of ANTEC, 1965; 14 (1-2): 77-89.

[34] Biron, M., Thermosets and Composites. 2004, Oxford: Elsevier.

[35] Jiri George Drobny, Applications of Thermal Elastomers. Handbook of Thermoplastic Elastomers, Second Edition, 2014, P301-337.

[36] Diaz J, Rubio L. Developments to manufacture structural aeronautical parts in carbon fiber reinforced thermoplastic materials. J Mater Process Technol 2003; 143-144:342-6.

[37] Cogswell, F. N., An introduction to thermoplastic composite materials. In thermoplastic Aromatic Polymer Composites. Butterworth-Heinemann, Oxford. 1992.

[37] Perng L.H., Thermal decomposition characteristics of poly(phenylene sulfide) by stepwise Py-GC/MS and TG/MS techniques. Polymer Degradation and Stability. 2000;(69): 323-332

[38] Jiri George Drobny, Applications of Thermal Elastomers. Handbook of Thermoplastic Elastomers, Second Edition, 2014, P301-337

[39] Manson JAE, Walkman MD, Bernet N. Composite processing and manufacturing-an overview. In: Comprehensive composite materials. Oxford, UK: Elsevier Science Ltd.; 200.p.577-607.

[40] Ning H, Vaidya U, Janowski GM, Husman G. Design, manufacture and analysis of a thermoplastic composites frame structure for mass transit. Composite Structure 2007; 80(1) 105-16.

[41] Diaz J, Rubio L. Developments to manufacture structural aeronautical parts in carbon fiber reinforced thermoplastic materials. J Mater Process Technol 2003; 143-144:342-6.

[42] Wang Q, Ning H, Vaidya U. Development of a carbonization-in-nitrogen method for measuring the fiber content of carbon fiber reinforced thermoset composites. Composites Part A, doi:10.1016/j.compositesa.2015.02.025

[43] Diaz J, Rubio L. Developments to manufacture structural aeronautical parts in carbon fiber reinforced thermoplastic materials. J Mater Process Technol 2003; (342-6):143-144

[44] Jiri G. D. Handbook of Thermoplastic Elastomers, Second Edition, 2014, P301-337